University of Tennessee, Knoxville
TRACE: Tennessee Research and Creative Exchange

Masters Theses | Graduate School

12-1984

Petrology of the Farmington Gabbro-Metagabbro Complex, North Carolina

James Thomas Harden
University of Tennessee, Knoxville

Follow this and additional works at: https://trace.tennessee.edu/utk_gradthes

Part of the Geology Commons

Recommended Citation

Harden, James Thomas, "Petrology of the Farmington Gabbro-Metagabbro Complex, North Carolina. " Master's Thesis, University of Tennessee, 1984.
https://trace.tennessee.edu/utk_gradthes/4366

This Thesis is brought to you for free and open access by the Graduate School at TRACE: Tennessee Research and Creative Exchange. It has been accepted for inclusion in Masters Theses by an authorized administrator of TRACE: Tennessee Research and Creative Exchange. For more information, please contact trace@utk.edu.

To the Graduate Council:

I am submitting herewith a thesis written by James Thomas Harden entitled "Petrology of the Farmington Gabbro-Metagabbro Complex, North Carolina." I have examined the final electronic copy of this thesis for form and content and recommend that it be accepted in partial fulfillment of the requirements for the degree of Master of Science, with a major in Geology.

Harry Y. McSween, Major Professor

We have read this thesis and recommend its acceptance:

Lawrence A. Taylor, Otto C. Kopp

Accepted for the Council:
Carolyn R. Hodges

Vice Provost and Dean of the Graduate School

(Original signatures are on file with official student records.)

To the Graduate Council:

I am submitting herewith a thesis written by James Thomas Harden entitled "Petrology of the Farmington Gabbro-Metagabbro Complex, North Carolina." I have examined the final copy of this thesis for form and content and recommend that it be accepted in partial fulfillment of the requirements for the degree of Master of Science, with a major in Geology.

H. Y. McSween, Major Professor

We have read this thesis and recommend its acceptance:

Accepted for the Council:

The Graduate School

PETROLOGY OF THE FARMINGTON GABBRO-METAGABBRO COMPLEX, NORTH CAROLINA

A Thesis

Presented for the

Master of Science

Degree

The University of Tennessee, Knoxville

James Thomas Harden

December 1984

ACKNOWLEDGMENTS

I would like to express my appreciation to Dr. Lawrence A. Taylor who provided guidance in the use of the electron microprobe, in compilation of data, and in the revision of the text; to Dr. Otto C. Kopp for his assistance in refining the details of the final draft; and especially to committee chairman Dr. Harry Y. McSween, Jr., who suggested the study area, provided guidance and support throughout this study, and assisted in revision of the text. I would also like to acknowledge Vulcan Materials for providing access to their quarry for the collection of samples.

Finally, I would like to thank my wife, Marsha, for spending many hours typing drafts and providing much needed moral support.

ABSTRACT

The Farmington gabbro-metagabbro complex is located along the western margin of the Charlotte belt of North Carolina. At least two or more intrusions occur within the complex. The Farmington gabbroic intrusion is postmetamorphic and contains plagioclase, hornblende, orthopyroxene, clinopyroxene, and olivine. Small amounts of magnetite, ilmenite, pyrite, pyrrhotite, pentlandite, hematite, hercynitic spinel, and biotite occur. Textures are hypidiomorphic granular to hypidiomorphic inequigranular. Four types of gabbroic rocks are present: hornblende gabbronorite, olivine-hornblende gabbronorite, hornblende norite, and olivine-hornblende norite, with olivine-hornblende gabbronorite predominating. A limited range of progressive differentiation is indicated by restricted increases in FeO/(FeO + MgO) ratios for mafic silicates and low anorthite contents of plagioclases.

The metamorphosed gabbroic intrusion surrounds the postmetamorphic gabbro. Four types of metagabbro can be distinguished based on mineralogy and texture: metagabbro protoliths, which have retained their original mineralogy and igneous textures; type I rocks, having relict igneous textures and clinopyroxene and/or olivine pseudomorphs; type II metagabbros, having poorly preserved igneous textures and minerals; and type III metagabbros, exhibiting textural and compositional banding. Types II and III are dominated by plagioclase and amphibole. Other minerals such as clinopyroxene and epidote may

occur along with titanite, magnetite, ilmenite, hematite, chlorite, biotite, and apatite. Type I rocks have substantially more clinopyroxene than type II and III samples, and metagabbro protoliths contain orthopyroxene and may contain olivine but no epidote. Hypidiomorphic granular to granoblastic textures occur.

A multiple intrusive history for the Farmington complex is suggested by xenoliths of metagabbro in gabbro, metagabbro xenoliths in metagabbro and lack of alteration of the gabbro. The metagabbro is composed of two or more intrusions as indicated by olivine-bearing and olivine-free metagabbro protolith, two distinct groups of igneous amphiboles, metagabbro xenoliths in metagabbro, and variability of metamorphic grade. The mineralogic differences and gneissic appearance would also support the presence of a layered intrusion.

Metamorphism ranges from greenschist to greenschist-lower amphibolite transitional grade. Metamorphism resulted in alteration of anhydrous mafic minerals and recrystallization. Variability may result from localized availability of H_2O, shearing, and repeated intrusion.

Gabbro-metagabbro complexes southwest of the study area are believed to have formed above an active subduction zone. Due to similarities and areal relationship with other complexes, the Farmington complex is suggested to have had the same origin. It has been suggested that these complexes represent "chimneys" formed by repeated intrusion which would heat the lithosphere and insulate successive magma bodies. The multiple intrusive nature of the Farmington complex would appear to support this model of emplacement.

TABLE OF CONTENTS

SECTION	PAGE
I. INTRODUCTION	1
II. FIELD AND ANALYTICAL METHODS	4
III. FIELD RELATIONS	6
Lithologic Units	6
Contact Relationships	10
Physical and Geophysical Expression	12
IV. PETROGRAPY AND MINERALOGY	15
Farmington Gabbro	15
Farmington Metagabbro	33
Areal Variations	43
V. PETROGENESIS	45
Emplacement as Multiple Intrusions	45
Metamorphism	45
Comparison with Other Mafic Complexes	47
Tectonic Setting	49
LIST OF REFERENCES	51
APPENDIX	57
VITA	64

LIST OF TABLES

TABLE		PAGE
1.	Modal Variations: Farmington Gabbroic Intrusion	16
2.	Representative Microprobe Analyses: Amphibole	17
3.	Representative Microprobe Analyses: Clinopyroxene	18
4.	Representative Microprobe Analyses: Olivine	19
5.	Representative Microprobe Analyses: Orthopyroxene	20
6.	Representative Microprobe Analyses: Plagioclase	21
7.	Modal Variations: Farmington Metagabbro	34
A-1.	Electron Microprobe Analyses (Averaged): Amphibole . . .	58
A-2.	Electron Microprobe Analyses (Averaged): Biotite	59
A-3.	Electron Microprobe Analyses (Averaged): Clinopyroxene .	60
A-4.	Electron Microprobe Analyses (Averaged): Olivine	61
A-5.	Electron Microprobe Analyses (Averaged): Orthopyroxene .	62
A-6.	Electron Microprobe Analyses (Averaged): Plagioclase . . .	63

LIST OF FIGURES

FIGURE		PAGE
1.	Location Map of Gabbro-Metagabbro Complexes in North Carolina	2
2.	Lithologic Map of the Farmington Gabbro-Metagabbro Complex, Davie County, North Carolina	7
3.	Simple Bouguer Gravity Map for Davie County, North Carolina	14
4.	Compositions of Coexisting Silicates for the Farmington Complex	22
5.	Calcic Amphibole Classification Diagram	25
6.	Plot of Al^{IV} Versus A-site Occupancy for Farmington, Barber, and Mecklenberg Ca-Amphiboles	26
7.	Plot Showing Variability of Al^{IV} Versus A-site + 2Ti + Al^{VI} + Fe^{3+}	27
8.	Petrologic Classification of Farmington Gabbro and Metagabbro Samples	30
9.	Photomicrographs of Farmington Gabbro	32
10.	Photomicrographs of Farmington Metagabbro	35
11.	Petrologic Areal Variations for the Farmington Gabbroic Intrusion	44

LIST OF PLATES

PLATE PAGE

1. Geologic Map of the Farmington Complex, North Carolina . . . . . In Pocket

I. INTRODUCTION

The southern Appalachian Piedmont contains more than thirty gabbroic intrusions (Butler and Ragland, 1969) that form a linear chain stretching from Georgia to North Carolina. Over the last twenty years many workers have attempted to explain the distribution, petrology, and relationship of these plutons to the evolution of the southern Piedmont. These studies range from limited petrographic reconnaissance (Butler, 1965, 1966; Cabaup, 1969; Chalcraft et al., 1978; Constantine-Herrera, 1971, Glover and Sinha, 1973; Hadley, 1973; Mathews, 1969; McCauley, 1961; McSween, 1970, 1980; Medlin, 1969b; Morgan, 1963; Myers, 1968; Wagener, 1974; Waskom and Butler, 1971), to detailed petrologic studies (Chalcraft, 1970; Clark, 1980; Deetz, 1980, Hermes, 1968; McSween and Nystrom, 1979; Medlin et al., 1972; Medlin, 1969a; Olsen, 1982). Several of these plutons within the Charlotte belt have associated metagabbro and amphibolite and form large mafic complexes. The linear chain formed by these gabbro-metagabbro-amphibolite complexes has been interpreted to have formed in a continental margin or island arc setting (Clark, 1980; McSween et al., 1984). The northernmost of these is the Farmington mafic complex located in Davie and Yadkin counties, North Carolina (Figure 1). This study will examine the Farmington gabbroic pluton and the metagabbro and amphibolite surrounding the pluton.

Comparisons will be drawn between the Farmington complex and two other complexes: the Mecklenburg complex and the Barber complex (Figure 1). The Farmington mafic complex is similar to the

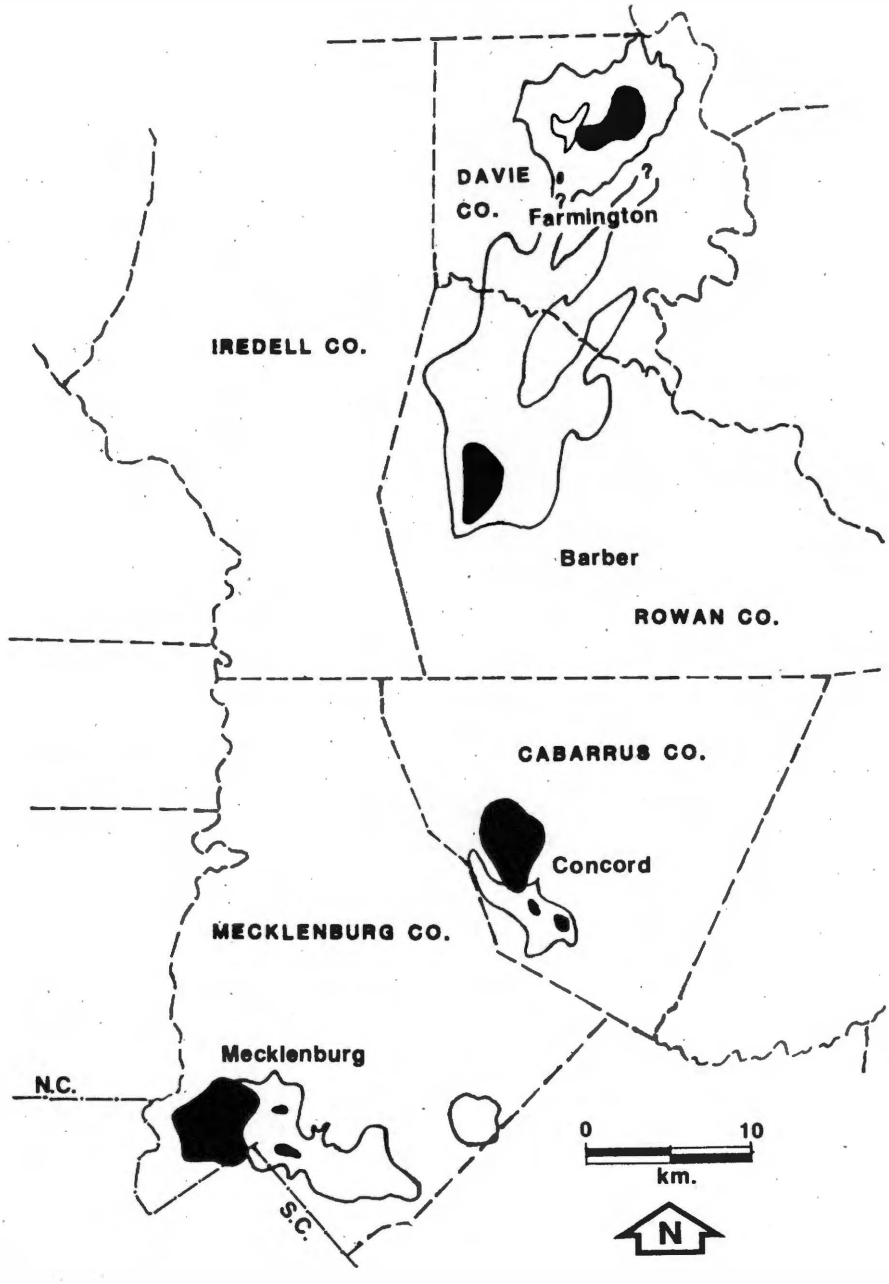

Figure 1. Location Map of Gabbro-Metagabbro Complexes in North Carolina. The Farmington complex is the most northerly complex in the chain. The metagabbro of the Farmington complex may be connected with the Barber metamorphosed intrusion.

Mecklenburg gabbro-metagabbro body south of Charlotte, North Carolina (Hermes, 1968); however, differences do exist. Generally the unmetamorphosed Farmington pluton tends to have less variation in modal percentages of minerals, and metamorphosed ultramafic rocks have not been reported associated with the Mecklenburg complex.

The Barber complex is located forty kilometers south of Farmington, and it has been suggested from regional gravity data (Wilson and Daniels, 1980) that the two complexes may be connected at depth. The metamorphosed Barber intrusion appears similar to the metamorphosed Farmington mafic rocks, but the unmetamorphosed Barber rocks are silica-saturated (Clark, 1980) and therefore are compositionally different from the postmetamorphic Farmington intrusion.

Many other similarities and differences exist between this complex and others in the chain. The information from this study may clarify the nature of the gabbro-metagabbro association and the relationship of the mafic complexes to each other.

II. FIELD AND ANALYTICAL METHODS

Topographic maps of the U.S.G.S. 1:24,000 scale series were utilized as base maps for geologic mapping (see Geologic Map in pocket). In addition, soil maps (Jurney and Bacon, 1927; U.S.D.A., 1978) and 1:250,000 scale geologic maps (Butler, 1978; Espenshade et al., 1975) aided mapping. Three hundred and eleven samples were collected from sample sites over a 114 square kilometer area. Samples were obtained from outcrops, large residual boulders, and float dug or plowed from fields. Metagabbro samples were also obtained from an active quarry. In areas where fresh rock was scarce or absent, saprolite or soil were used as indicators of rock type. The rust-brown to grayish-brown color of the Mecklenburg and Iredell soils series are indicative of the weathering of mafic and ultramafic rocks, whereas the weathering of intermediate and granitic rocks produces red and grayish-yellow soils of the Davidson, Cecil, and Wilkes soils series (Jurney and Bacon, 1927). These soil-rock associations provided a good indication of the approximate location of contacts between country rocks and mafic rocks. The locations of contacts between metagabbro and gabbro were estimated by sampling all available outcrop and float near possible contacts.

Thin sections were prepared for ninety-two samples. Twenty-six gabbros and twenty-one metagabbros were point counted to determine modal percentages of minerals. The number of points counted ranged from 1,000-1,900. The accuracy of point counting depends on such analytical variables as fabric, texture, counting interval and grain

size, which can increase analytical error and make variance difficult to estimate (Chayes, 1956; Neilson and Brockman, 1977). These variables may have influenced the modal analyses, but a minimum value for the absolute and relative error can be estimated based on the number of points counted (Van der Plas and Tobi, 1965). Generally, the absolute error is ±1 to 3%, and relative error ranges from ±4 to 28% for the major constituents.

Mineral analyses were performed using a MAC 400S automated electron microprobe with appropriate synthetic and natural standards. Matrix corrections were made according to the method of Bence and Albee (1968) using the data of Albee and Ray (1970). Voltage was maintained at 15 kv and a beam current was between 0.04 and 0.05 μa. The beam current was monitored by a graphite flag and corrected for "drift." Major minerals were analyzed in eleven polished thin sections using a partially defocused electron beam with a diameter of approximately 5 μm to 15 μm. Beam currents of 0.04 μa were used for plagioclase and hornblende analyses, 0.045 μa for pyroxene analyses, and 0.49 μa for olivine analyses. Representative analyses are presented in Section 4; averages for all analyses and standard deviations are presented in the Appendix. FeO was recalculated for amphibole analyses to obtain percentages of Fe^{2+} and Fe^{3+} in oxide phases based on charge and stoichiometry (Taylor, 1978). Al^{IV} and Al^{VI} were calculated by the method set forth by Leake (1978).

III. FIELD RELATIONS

Lithologic Units

The study area is located within the Charlotte belt of the North Carolina Piedmont in northeastern Davie County (Figure 2). The Charlotte belt has the greatest concentration of intrusions of any belt in the Piedmont (Butler and Ragland, 1969), ranging in composition from felsic to ultramafic (Fullagar, 1971). Regional metamorphic grade is generally amphibolite facies locally retrograded to greenschist facies (Butler and Fullagar, 1978).

The country rocks surrounding the Farmington complex are comprised of schists, gneisses, and sedimentary rocks. In the study area, schistose rocks are composed predominantly of fine- to medium-grained quartz-muscovite schists with units of biotite schist and biotite-quartz-feldspar gneiss. Poikiloblastic cordierite containing quartz and needles of sillimanite is found occasionally in the quartz-muscovite schist. The presence of sillimanite is apparently anomalous with the regional trend northeast of the study area. Kyanite is known to occur in the western half of the Charlotte belt, whereas sillimanite occurs in the eastern half (Espenshade et al., 1975). Since the location of the Farmington complex is along the western margin of the Charlotte belt (Figure 2), the occurrence of sillimanite either indicates a higher regional metamorphic grade for the western portion of the Charlotte belt in this vicinity or is the result of contact metamorphism by the gabbroic intrusions.

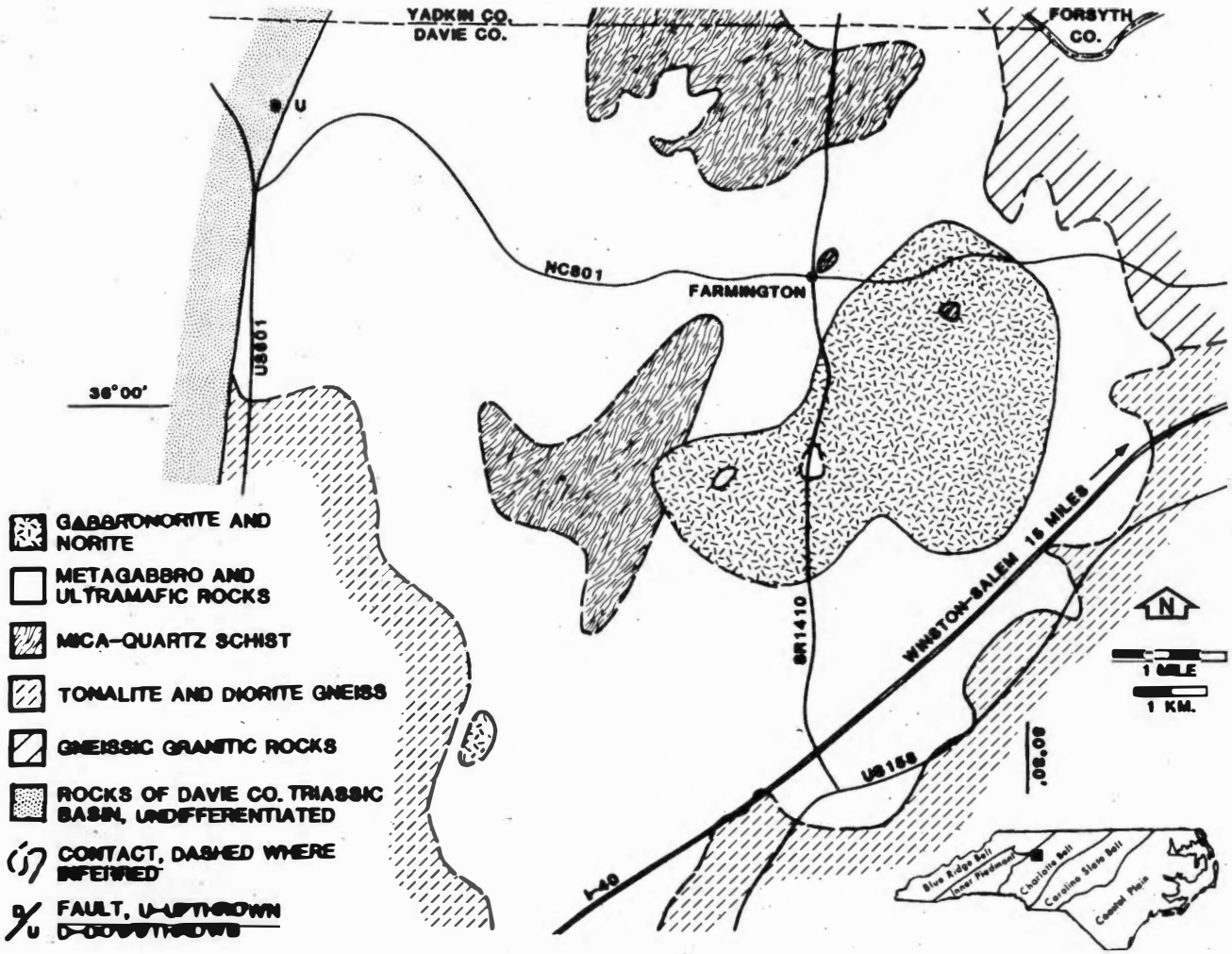

Figure 2. Lithologic map of the Farmington gabbro-metagabbro complex, Davie County, North Carolina. The study area, represented as a black square on the North Carolina map, is located near the western margin of the Charlotte belt.

Metamorphosed igneous lithologies are the most common country rocks. Fine- to very coarse-grained gneissic adamellite and granodiorite are generally composed of biotite, muscovite, epidote, and large microcline phenocrysts with garnet and hornblende being locally abundant. Fine- to medium-grained metatonalites and metadiorites consist mainly of euhedral and subhedral plagioclase and subhedral biotite with minor amounts of subhedral hornblende and anhedral quartz. The development of foliation is weak and dependent on the amount of biotite.

Unmetamorphosed diabase, pegmatite, and granite are found within the study area. Diabase is by far the most common. These Mesozoic diabase dikes are subophitic, fine- to medium-grained rocks containing plagioclase, olivine, and clinopyroxene. Pegmatites of uncertain age are predominantly microcline and quartz with minor amounts of muscovite, biotite, hornblende, and garnet. Graphic intergrowths of microcline and quartz are common. A small, postmetamorphic granite occurs at the edge of the study area and the large Churchland granite, a Salisbury type pluton, occurs several miles southeast of the Farmington complex (Butler, 1978; Butler and Ragland, 1969; Butler and Fullagar, 1978; Fullagar, 1971).

Sedimentary rocks of Triassic age occurring in the study area have been mapped and described by Thayes (1967, 1970). These rocks consist of conglomerates, sandstones, siltstones, and claystones.

The Farmington complex can be subdivided into metamorphosed ultramafic rocks, metamorphosed gabbroic rocks, and unmetamorphosed

gabbroic rocks. The predominant ultramafic rock type is hornblendite. It is made up of large hornblende oikocrysts containing amphibole pseudomorphs of pyroxenes which frequently exhibit relict zoning and contain zonally included opaques. An amphibolite grade event and a retrograde event affect all hornblendites. The amphibolite grade event produced hornblende after pyroxene, whereas retrogradation resulted in the production of pale green to colorless actinolite, pale green chlorite, and green to bluish-green hornblende. The greenschist event varies widely in intensity and in some cases is dependent on shearing. Actinolite and chlorite amount to only a few percent in unsheared rocks to approximately 95% in the mylonitized hornblendites. Sheared hornblendites form fine-grained chlorite-actinolite schists with ragged hornblende porphyroblasts. An occurrence of serpentinized periodotite is found in the southwestern corner of the complex. Relict serpentinized grains are set in a matrix of fibrous serpentine and fine-grain opaques.

The fine- to coarse-grained metamorphosed gabbroic lithologies are dominated by plagioclase and amphibole. Clinopyroxene, orthopyroxene, olivine, biotite, quartz, epidote, and chlorite occur depending on the degree of alteration. Generally, exposures show a foliation of the plagioclase and mafic grains and, in some cases, the outcrop exhibits a gneissic appearance and layering. Whether or not this fabric is a result of igneous processes or metamorphic mineral segregation could not be determined in the field. Shearing occurs in a few outcrops. In one case, evidence for two episodes of shearing was

observed. The more steeply dipping shears are cut and deformed by later shears. The cataclastic rocks were usually retrograded to chlorite or talc-anthophyllite schists. In instances where retrogradation did not take place the rocks consist of plagioclase, hornblende, and quartz with flaser texture.

Plagioclase, orthopyroxene, clinopyroxene, hornblende, and olivine with minor amounts of biotite and opaques make up the primary mineral assemblage of the unmetamorphosed gabbro. These medium- to coarse-grained rocks outcrop as large spheroidal boulders and as saprolite.

Contact Relationships

The contacts between gabbro, metagabbro, and country rocks were not directly observed in the field. Approximate location of a contact was determined by abrupt changes in soil, saprolite, and float. Metagabbro, poorly exposed over approximately 45 km^2, has contacts with all major rock types in the study area except postmetamorphic granites (Figure 2). These granites intrude the metatonalites and metadiorites that border the complex on the south. Small xenoliths of metatonalite are present in the metamorphosed gabbro and range in size from a few millimeters to a few centimeters.

The western margin of the complex is marked by a fault which brings Triassic age sediments in contact with mylonitized metagabbro and ultramafic rocks. These sedimentary rocks are shown by Espenshade and others (1975) to overlie chlorite schists that outcrop

as small inliers in the basin. Mylonitization of mafic and ultramafic rocks within the Farmington complex occurs in a 50 to 100 meter-wide zone parallel to the fault. The mylonitization produced a strongly foliated talc-anthophyllite-chlorite schist with foliation parallel to faulting.

The quartz-muscovite schist, biotite schist, and biotite-quartz-feldspar gneiss border the complex on the north. Two pods of the quartz-muscovite schist occur within the metamorphosed gabbroic rocks (Figure 2), and it could not be determined in the field whether these pods represent xenoliths, roof pendants, or infolded material. Within the unmetamorphosed gabbroic pluton a xenolith or roof pendant of this quartz-muscovite schist was also found.

The eastern side of the complex is bounded by gneissic adamellite and granodiorite. According to Espenshade and others (1975), these plutonic rocks usually become nonfoliated away from their contacts, but this was not observed in the study area. Based on previous mapping by Espenshade and on the mapping in this study, it appears that the metagabbro intrudes these gneisses.

Mesozoic diabase dikes (Espenshade et al., 1975; Ragland et al., 1968), pegmatites of uncertain age, and veins of both felsic and mafic compositions crosscut all major rock types in the study area. Many diabase dikes can be traced for some distance by following residual boulder trains.

Contacts in saprolite reveal that ultramafic rocks intrude the metagabbroic rocks as sill-like bodies. While some veins cut both rock

types, many veins which crosscut metagabbro are truncated at the ultramafic contacts. The principle occurrence of ultramafic rocks is in the northern part of the Farmington complex.

The most unusual and unexpected contact observed was in a fine-grained metagabbro containing millimeter scale xenoliths of a coarse-grained metagabbro of similar mineralogy. This metagabbro-metagabbro contact signifies that more than one metagabbro intrusion is present within the complex.

The unmetamorphosed gabbroic pluton, covering an area of 11 km^2 within the complex, has an elongate outcrop trending northeast-southwest. A small satellite pluton outcrops in the southwestern corner of the complex. Two metagabbro xenoliths or roof pendants occur within the larger gabbro. Gabbro-metagabbro contacts were never directly observed; however, a traverse across a supposed meta-gabbro contact with gabbro yielded "in place" residual rock from saprolite. The fresh residual gabbro and metagabbro samples were separated by no more than 10 meters. The presence of the two rock types in such close association seems to refute the possibility that the unaltered gabbro is a remnant of the metamorphosed gabbro.

Physical and Geophysical Expression

Gabbroic plutons in the Piedmont typically show a correlation between topography and rock type (e.g., Chalcraft, 1970; Deetz, 1980; McSween and Nystrom, 1979), and this relationship is evident in the study area. Slope is gentle and relief is no greater than 120 feet

in areas underlain by gabbro. In areas where metagabbro and hornblendite occur, slope is gentle to moderate and relief is approximately 200 feet. Relief outside the complex ranges as high as 250 feet and slopes are generally moderate. The quartz-muscovite schist xenolith within the gabbro forms a prominent steep-sided hill in marked contrast to the gently rolling terrain of the pluton.

Positive gravity anomalies in the Charlotte belt are generally associated with mafic intrusions (Chalcraft, 1970; Clark, 1980; Morgan, 1963), and the Farmington complex is no exception to this association. Simple Bouguer gravity data (Wilson and Daniels, 1980; Taylor, 1982) indicate a gravity high over the Farmington complex (Figure 3) and a gravity ridge extending south to another positive gravity anomaly over the Barber complex. This may suggest that the two complexes are connected at depth. In addition, an aeromagnetic high is found to occur over the Farmington complex (Melton, 1980).

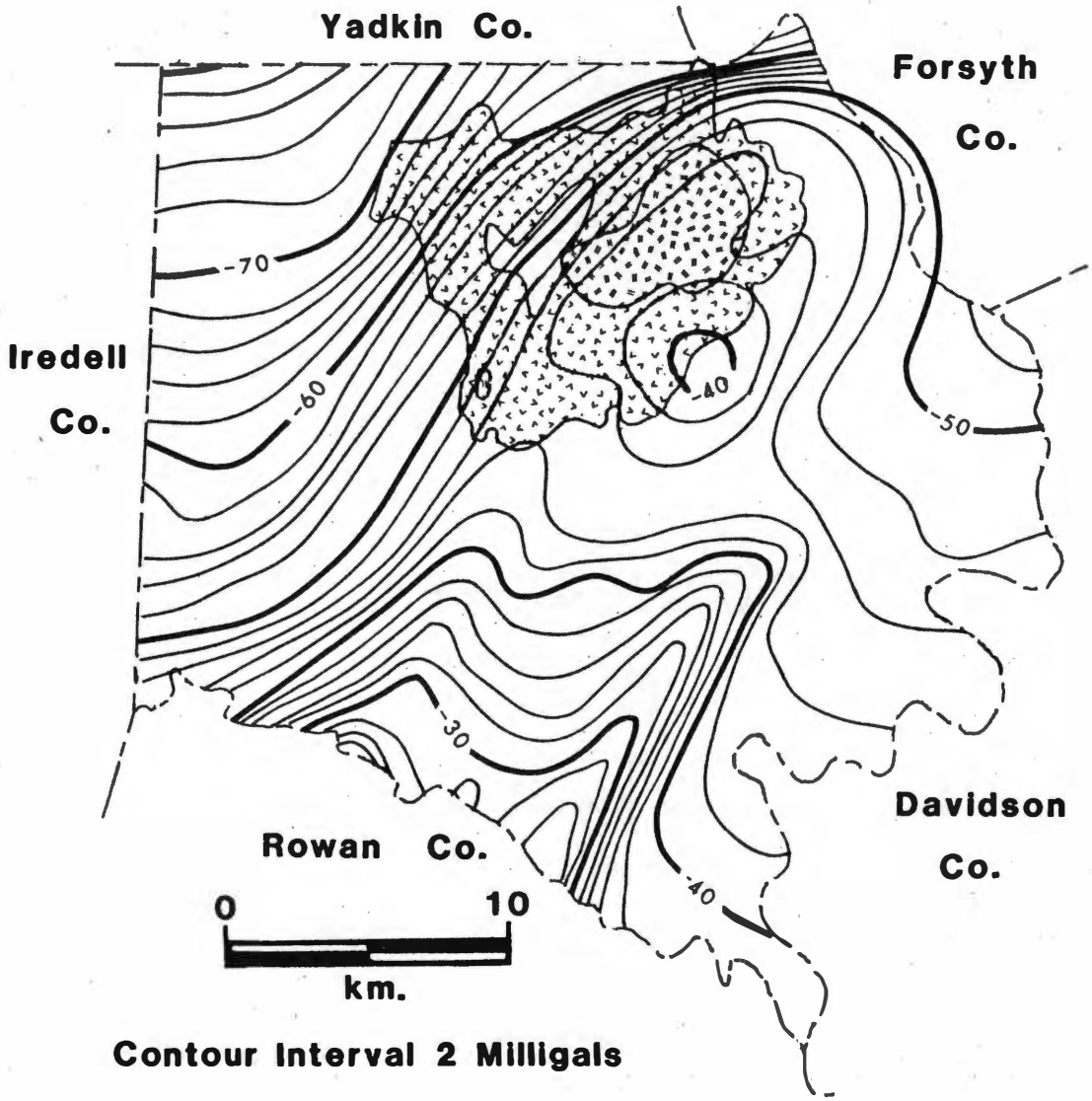

Figure 3. Simple Bouguer Gravity Map for Davie County, North Carolina (from Wilson and Daniels, 1980). The Farmington complex corresponds to the positive Bouguer anomaly in northern Davie County. The edge of another positive anomaly occurs southeast of the Famington complex which corresponds to the Barber complex in Rowan County.

IV. PETROGRAPHY AND MINERALOGY

Farmington Gabbro

The Farmington Gabbro is composed primarily of plagioclase, olivine, orthopyroxene, clinopyroxene and hornblende. Minor amounts of biotite, apatite, serpentine, chlorite, hercynitic spinel, and sericite are present as well as opaque minerals (magnetite, ilmenite, pyrrhotite, pentlandite, pyrite, and hematite). Modal percentages of minerals are presented in Table 1. Tables 2-6 present representative analyses of major minerals.

Plagioclase is the most abundant mineral in the pluton (54.1-73.5%) and forms subhedral, medium- to coarse-grained crystals. Oriented rodlets of opaques and other minerals occur in many plagioclase grains. Anorthite contents range from An_{50} to An_{68}, and traverses reveal faint to moderate normal zoning and in one traverse, oscillatory zoning.

The gabbro contains 0.2 to 17.3% of anhedral to subhedral olivine. The olivine composition ranges from Fo_{71} to Fo_{82} (Figure 4), but individual grains lack zoning and are generally uniform within a section. Fractures in olivine are often filled with serpentine and/or magnetite. Serpentine and orthopyroxene ± opaques or serpentine alone partially replace olivine or form pseudomorphs of olivine. Reaction rims of orthopyroxene and amphibole are common. A few samples from the northern portion of the pluton display corona development on olivine grains. The coronas consist of an outer rim of

Table 1. Modal Variations: Farmington Gabbroic Intrusion

	PLG	OPX	CPX	OLV	HBL	OPA	BIO	FIB AMP	SERC	SERP	CHL	AP	HER
F-1	60.0	16.7	2.9	1.6	14.2	2.0	0.9	T	0.5	0.5	0.5	0.1	T
F-2	63.0	10.8	10.9	6.2	6.3	1.3	T	0.3	0.3	0.8	T	T	0.1
F-3	63.7	12.5	5.7	1.7	10.8	2.5	0.4	T	0.8	1.9	0.1	T	T
F-4	73.5	8.2	2.4	5.3	7.5	0.4	0.4	1.0	0.6	0.4	0.3	0.3	T
12-1	59.4	15.1	9.2	0.2	10.0	1.3	0.2	2.9	0.5	0.5	0.4	0.3	T
12-11	63.2	7.5	5.3	12.8	4.7	2.9	T	2.8	0.6	0.1	-	-	0.1
3-15-11	65.0	11.3	4.3	11.7	5.8	1.2	T	-	0.3	0.2	-	-	0.1
4-21-9	68.8	13.4	2.1	5.6	7.6	1.0	0.6	0.1	0.4	0.4	-	-	T
4-21-10	66.8	6.4	2.5	11.3	9.5	0.7	0.4	1.5	0.4	0.3	0.1	0.1	0.1
5-9-1	66.8	12.2	5.2	4.6	7.2	2.2	0.4	-	0.3	0.4	0.1	0.3	0.1
5-9-4	63.9	14.2	7.0	5.1	5.6	3.0	0.1	T	0.5	0.5	0.1	T	T
5-10-3	65.8	13.4	8.7	5.3	4.7	1.0	0.1	-	0.2	0.5	0.1	-	0.2
5-10-4	61.0	10.3	4.9	13.1	9.0	0.5	0.2	0.1	0.3	0.4	0.1	-	0.1
5-10-6	56.9	19.3	13.6	1.5	5.5	2.0	T	-	0.1	0.9	-	0.2	T
6-11-8	54.1	13.4	6.9	1.0	21.8	1.3	0.3	-	0.1	0.7	0.1	0.3	T
6-13-3	67.8	5.6	6.6	14.6	4.2	0.8	T	-	0.3	0.1	-	-	T
6-13-4	57.3	13.6	13.2	2.2	10.1	2.3	0.1	-	0.2	0.6	0.4	0.1	T
6-13-6	62.5	9.7	12.3	7.1	5.2	2.3	0.1	-	0.1	0.6	0.1	-	T
6-13-7	65.1	6.5	5.5	16.7	4.5	0.7	T	-	0.4	0.6	T	-	T
6-13-8	63.8	10.9	6.3	3.5	11.2	1.5	0.3	-	0.5	1.8	0.2	0.1	T
6-14-8	61.4	12.1	9.8	8.9	3.9	1.3	T	1.6	0.5	0.3	0.1	-	0.2
6-14-10	69.9	6.1	0.6	17.3	1.6	0.8	0.2	2.4	0.4	0.5	0.2	-	T
6-14-13	64.3	6.4	9.0	8.9	7.2	2.5	0.1	0.2	0.5	0.3	0.2	0.1	0.2
6-15-3	55.5	11.0	3.2	4.7	6.9	1.4	0.2	15.0	0.8	0.1	1.2	0.2	T
6-15-4	66.4	11.0	1.8	7.3	10.4	1.8	0.6	-	0.2	0.1	0.2	0.2	0.1
6-15-5	61.3	5.7	12.3	10.5	4.3	2.2	0.3	2.2	0.6	0.3	0.1	-	0.3

Table 2. Representative Microprobe Analyses: Amphibole

	3-15-3[b]	5-10-6	6-11-8	6-13-8	6-14-10	6-15-4	6-15-5	8-4-5[b]	9-6Q-5A[b]	9-6Q-7A[b]	9-6Q-7C[b]
SiO_2	41.4	41.7	42.4	41.2	42.1	40.6	42.1	41.5	45.0	45.7	43.4
TiO_2	3.03	4.26	1.54	3.75	2.45	3.68	4.01	2.12	2.35	1.34	2.48
Al_2O_3	12.7	12.7	13.3	13.3	13.5	12.4	12.5	13.4	10.8	8.27	10.5
FeO	5.43	8.36	3.60	5.89	5.75	8.08	8.47	1.90	6.84	12.9	4.79
Fe_2O_3[a]	5.82	2.77	8.92	3.90	4.30	4.23	2.54	8.58	5.65	3.79	5.59
MnO	0.14	0.18	0.19	0.16	0.14	0.14	0.14	0.17	0.14	0.61	0.09
MgO	14.1	13.7	15.2	14.8	14.2	13.3	13.5	15.6	13.9	11.6	14.7
CaO	11.5	11.4	12.0	11.7	11.6	11.2	11.2	11.9	11.7	11.5	11.5
Na_2O	2.13	2.79	2.43	2.72	2.45	2.62	2.70	2.09	1.15	1.55	1.14
K_2O	0.88	0.82	0.96	0.82	1.16	1.05	0.81	0.65	0.86	1.04	0.93
Total	97.13	98.68	100.54	98.24	97.65	97.30	97.97	97.91	98.39	98.30	95.12
					Atoms/23 (O, OH, F)						
Si	6.057	6.049	6.004	5.969	6.129	6.014	6.143	5.970	6.470	6.763	6.418
Ti	0.333	0.465	0.164	0.409	0.268	0.410	0.440	0.229	0.254	0.149	0.276
Al^{IV}	1.943	1.951	1.996	2.031	1.871	1.986	1.857	2.030	1.530	1.237	1.582
Al^{VI}	0.252	0.221	0.221	0.236	0.451	0.178	0.288	0.248	0.309	0.206	0.246
Fe^{2+}	0.664	1.015	0.427	0.714	0.700	1.000	1.033	0.229	0.823	1.591	0.593
Fe^{3+}	0.641	0.303	0.951	0.425	0.471	0.471	0.279	0.929	0.612	0.422	0.623
Mn	0.017	0.022	0.023	0.020	0.017	0.018	0.017	0.021	0.017	0.076	0.011
Mg	3.084	2.974	3.214	3.196	3.091	2.924	2.943	3.344	2.978	2.555	3.252
Ca	1.799	1.774	1.822	1.812	1.760	1.778	1.742	1.841	1.801	1.828	1.824
Na	0.604	0.786	0.668	0.764	0.672	0.752	0.763	0.583	0.321	0.445	0.854
K	0.164	0.152	0.174	0.152	0.210	0.198	0.151	0.119	0.158	0.196	0.458
Total	15.558	15.712	15.664	15.728	15.640	15.729	15.656	15.543	15.273	15.468	16.137

[a] Fe_2O_3 calculated.

[b] Metagabbro samples. Analyses are for igneous amphiboles.

Table 3. Representative Microprobe Analyses: Clinopyroxene

	3-15-3[b]	5-10-6	6-11-8	6-13-8	6-14-10	6-15-4	6-15-5	8-4-5[b]	9-6Q-5A[b]	9-6Q-7A[b]	9-6Q-7C[b]
SiO_2	50.6	51.4	51.8	51.8	50.9	50.6	51.4	50.1	53.1	52.4	51.2
TiO_2	0.70	0.80	0.62	0.80	0.76	0.61	0.78	0.52	0.31	0.22	0.66
Al_2O_3	4.22	3.93	3.43	3.96	4.42	2.77	3.55	4.57	2.11	1.93	3.49
FeO[a]	7.36	6.91	7.87	7.10	7.10	8.45	7.00	7.95	7.68	9.19	7.74
MnO	0.21	0.22	0.28	0.17	0.21	0.34	0.18	0.27	0.17	0.84	0.09
MgO	15.8	14.6	15.5	14.6	14.7	15.1	14.5	15.6	15.1	14.4	14.7
CaO	19.7	21.6	20.1	20.3	20.9	20.9	21.7	19.6	21.5	20.3	20.8
Na_2O	0.64	0.69	0.59	0.71	0.59	0.60	0.67	0.47	0.44	0.70	0.61
Total	99.23	100.18	100.19	99.44	99.58	99.37	99.78	99.08	100.41	99.98	99.29
						Atoms/6 Oxygen					
Si	1.877	1.898	1.909	1.916	1.889	1.897	1.906	1.870	1.955	1.953	1.911
Ti	0.020	0.021	0.016	0.021	0.021	0.016	0.021	0.014	0.008	0.005	0.017
Al	0.184	0.170	0.148	0.171	0.192	0.122	0.154	0.200	0.090	0.084	0.153
Fe	0.227	0.212	0.242	0.219	0.220	0.264	0.216	0.247	0.235	0.285	0.241
Mn	0.006	0.006	0.008	0.004	0.006	0.010	0.005	0.007	0.005	0.026	0.002
Mg	0.873	0.801	0.848	0.803	0.811	0.846	0.801	0.867	0.828	0.799	0.815
Ca	0.781	0.854	0.793	0.803	0.829	0.840	0.859	0.785	0.848	0.812	0.832
Na	0.045	0.048	0.041	0.050	0.041	0.042	0.048	0.034	0.031	0.050	0.043
Total	4.013	4.010	4.005	3.987	4.007	4.037	4.010	4.024	4.000	4.014	4.014

[a]FeO = Total Fe.

[b]Metagabbro samples.

Table 4. Representative Microprobe Analyses: Olivine

	5-10-6	6-11-8	6-13-8	6-14-10	6-15-4	6-15-5	8-4-5[b]
SiO_2	37.9	38.5	37.6	38.3	36.3	37.7	38.1
FeO[a]	23.9	16.9	20.1	22.1	26.4	23.5	17.5
MnO	0.61	0.35	0.27	0.42	0.42	0.47	0.36
MgO	37.3	44.6	42.2	39.1	36.9	38.2	44.0
Total	99.71	100.35	100.17	99.92	100.02	99.87	99.96
				Atoms/4 Oxygens			
Si	0.998	0.976	0.969	0.996	0.967	0.989	0.973
Fe	0.526	0.357	0.433	0.479	0.588	0.515	0.373
Mn	0.009	0.007	0.005	0.009	0.009	0.010	0.007
Mg	1.459	1.684	1.621	1.518	1.466	1.493	1.673
Total	2.992	3.024	3.028	3.002	3.030	3.007	3.026

[a]FeO = Total Fe.

[b]Metagabbro sample.

Table 5. Representative Microprobe Analyses: Orthopyroxene

	5-10-6	6-11-8	6-13-8	6-14-10	6-15-4	6-15-5	8-4-5[b]	9-6Q-7C[b]
SiO_2	53.6	53.7	54.2	53.8	53.6	55.3	53.3	53.7
TiO_2	0.27	0.05	0.12	0.18	0.32	0.39	0.21	0.19
Al_2O_3	2.11	2.07	2.86	2.79	1.96	1.91	2.95	1.70
FeO[a]	15.1	14.0	14.1	14.0	17.0	14.9	14.2	19.6
MnO	0.53	0.45	0.32	0.43	0.44	0.43	0.29	0.51
MgO	27.5	29.3	28.1	28.6	26.7	28.2	28.1	24.7
CaO	1.25	0.77	0.67	0.79	1.02	0.83	1.23	0.58
Total	100.36	100.34	100.37	100.59	101.04	101.96	100.28	100.98
				Atoms/6 Oxygens				
Si	1.929	1.920	1.931	1.918	1.929	1.947	1.909	1.953
Ti	0.006	0.001	0.003	0.004	0.008	0.010	0.005	0.004
Al	0.088	0.087	0.120	0.117	0.082	0.078	0.124	0.072
Fe	0.453	0.418	0.420	0.416	0.512	0.438	0.424	0.595
Mn	0.016	0.012	0.009	0.012	0.012	0.012	0.008	0.015
Mg	1.474	1.561	1.491	1.519	1.434	1.480	1.500	1.339
Ca	0.047	0.029	0.025	0.029	0.039	0.031	0.046	0.022
Total	4.013	4.028	3.999	4.015	4.016	3.996	4.016	4.000

[a]FeO = Total Fe.

Table 6. Representative Microprobe Analyses: Plagioclase

	3-15-3[b]	5-10-6	6-11-8	6-13-8	6-14-10	6-15-4	6-15-5	8-4-5[b]	9-6Q-5A[b]	9-6Q-7A[b]	9-6Q-7C[b]
SiO_2	52.4	55.1	52.7	52.6	52.4	54.8	53.1	47.1	54.2	61.3	53.0
Al_2O_3	29.8	28.7	30.6	30.4	29.9	29.4	29.6	33.7	28.7	24.8	30.0
CaO	12.6	10.9	12.2	12.0	12.0	11.2	11.6	16.4	11.1	6.41	12.1
Na_2O	4.09	4.91	4.42	4.41	4.38	4.69	4.75	1.89	0.01	7.61	4.63
K_2O	0.04	0.20	0.15	0.18	0.13	0.21	0.07	N.D.[c]	0.05	0.23	0.23
FeO[a]	0.22	0.11	0.27	0.32	0.15	0.14	0.20	0.41	0.11	0.07	0.25
Total	99.35	99.92	100.34	99.91	98.96	100.44	99.31	99.50	99.17	100.42	100.21
						Atoms/8 Oxygens					
Si	2.393	2.482	2.379	2.383	2.394	2.458	2.416	2.172	2.459	2.710	2.397
Al	1.604	1.521	1.626	1.624	1.609	1.551	1.587	1.829	1.535	1.292	1.598
Ca	0.614	0.526	0.588	0.583	0.588	0.539	0.566	0.810	0.539	0.303	0.586
Na	0.362	0.429	0.387	0.387	0.387	0.408	0.418	0.167	0.439	0.651	0.406
K	0.001	0.010	0.008	0.009	0.006	0.012	0.002	0.000	0.002	0.013	0.012
Fe	0.008	0.004	0.009	0.012	0.005	0.005	0.006	0.015	0.004	0.001	0.009
Total	4.982	4.972	4.997	4.998	4.989	4.973	4.993	4.993	4.978	4.970	5.008

[a]FeO = Total Fe.

[b]Metagabbro samples.

[c]N.D.--not detected, less than 0.03%.

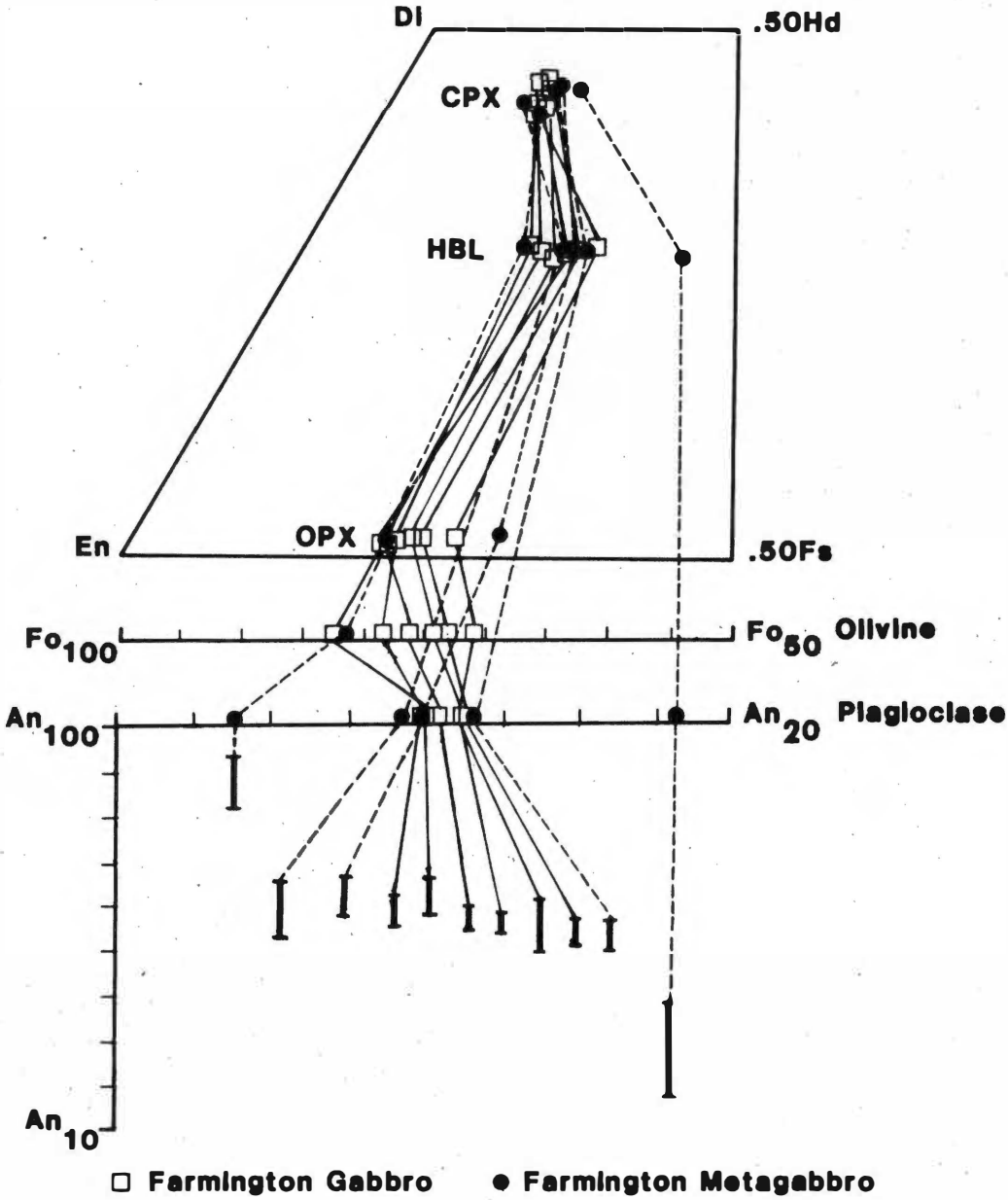

Figure 4. Compositions of Coexisting Silicates (in mole %) for the Farmington Complex. Tie-lines connect coexisting phases and bars indicate the range of anorthite content for plagioclase. Farmington metagabbro samples show a broader range in plagioclase anorthite content and Fe content for mafic silicates than the unmetamorphosed gabbro samples. Hornblende compositions are projected in terms of Ca, Mg, and Fe.

radially fibrous amphibole with vermicular inclusions of spinel in contact with plagioclase and an inner rim of radially fibrous or prismatic orthopyroxene bordering olivine. Development of coronas is apparently related to microfractures that allowed fluids to be introduced. Coronas decrease in thickness as distance from fractures increases and olivine grains most distant from fractures lack coronas. The introduction of fluid under regional metamorphic conditions has been cited by some authors as necessary for corona development (Murty, 1958; Stramer, 1969), but Esbensen (1978) and Sapountzis (1975) have shown that regional metamorphism is not necessary and deuteric alteration or autometamorphism may be responsible. Lack of any alteration of other mafic grains and the absence of coronas in other samples tends to support the later processes.

Orthopyroxene (5.6-19.3%) occurs as large, faintly pleochroic (green to pink) oikocrysts containing plagioclase, olivine, and clinopyroxene, and in reaction relationship with olivine. The composition ranges from $Wo_1En_{78}Fs_{21}$ to $Wo_2En_{72}Fs_{26}$ (Figure 4). Exsolution lamellae of clinopyroxene parallel to (100) are common, whereas exsolved ilmenite rodlets parallel to (010) and (001) are rare to infrequent. Symplectic intergrowth of orthopyroxene and magnetite plus minor ilmenite are commonly associated with olivine. These intergrowths grade from coarse to fine toward the olivine. The formation of these intergrowths is probably a result of the reaction of olivine with liquid (Ambler and Ashley, 1977; McSween, 1980) or by direct precipitation (Garrison and Taylor, 1981).

Clinopyroxene (0.6-13.6%) forms pale green to gray poikilitic grains enclosing plagioclase and olivine and, rarely, as discrete subhedral grains. Clinopyroxene shows exsolution of orthopyroxene along (100) and oxides (magnetite and ilmenite) parallel to (100) and (010). Opaque minerals tend to be concentrated in the interior of the clinopyroxene grains leaving somewhat clear margins. Bands of inclusions in the (001) sections are limited to interlamellar areas and their arrangement is restrained by the (100) orthopyroxene lamellae, which suggests that the inclusions postdate the orthopyroxene exsolution. These inclusions are similar to ones found in augites in the Umfraville gabbro in eastern Ontario (Fleet et al., 1980) and in other gabbros in the southeast Piedmont (see McSween, 1980). The composition of clinopyroxene in the Farmington gabbro is augite (Figure 4).

Amphibole, pleochroic from straw yellow or yellow-brown to reddish-brown, occurs as oikocrysts, and in reaction relationship rimming pyroxenes, ilmenite, and magnetite. It is also found as pleochroic colorless to green, fibrous coronas (previously discussed). Rods and plates of ilmenite are found in some oikocrysts. The compositions of the amphiboles are plotted in Figure 4 on the basis of their Ca-Mg-Fe contents. Using the classification of Leake (1978), most amphiboles are classified as magnesio-hastingsites (Figure 5), although two analyzed grains are paragasite. Plots of Al^{IV} versus $(Na + K)_A$ (Figure 6) and Al^{IV} versus total A-site occupancy including $Al^{VI} + 2Ti + Fe^{3+}$ (Figure 7) reveal that a paragasite-hastingsite type substitution accounts for most of the variability in A-site occupancy.

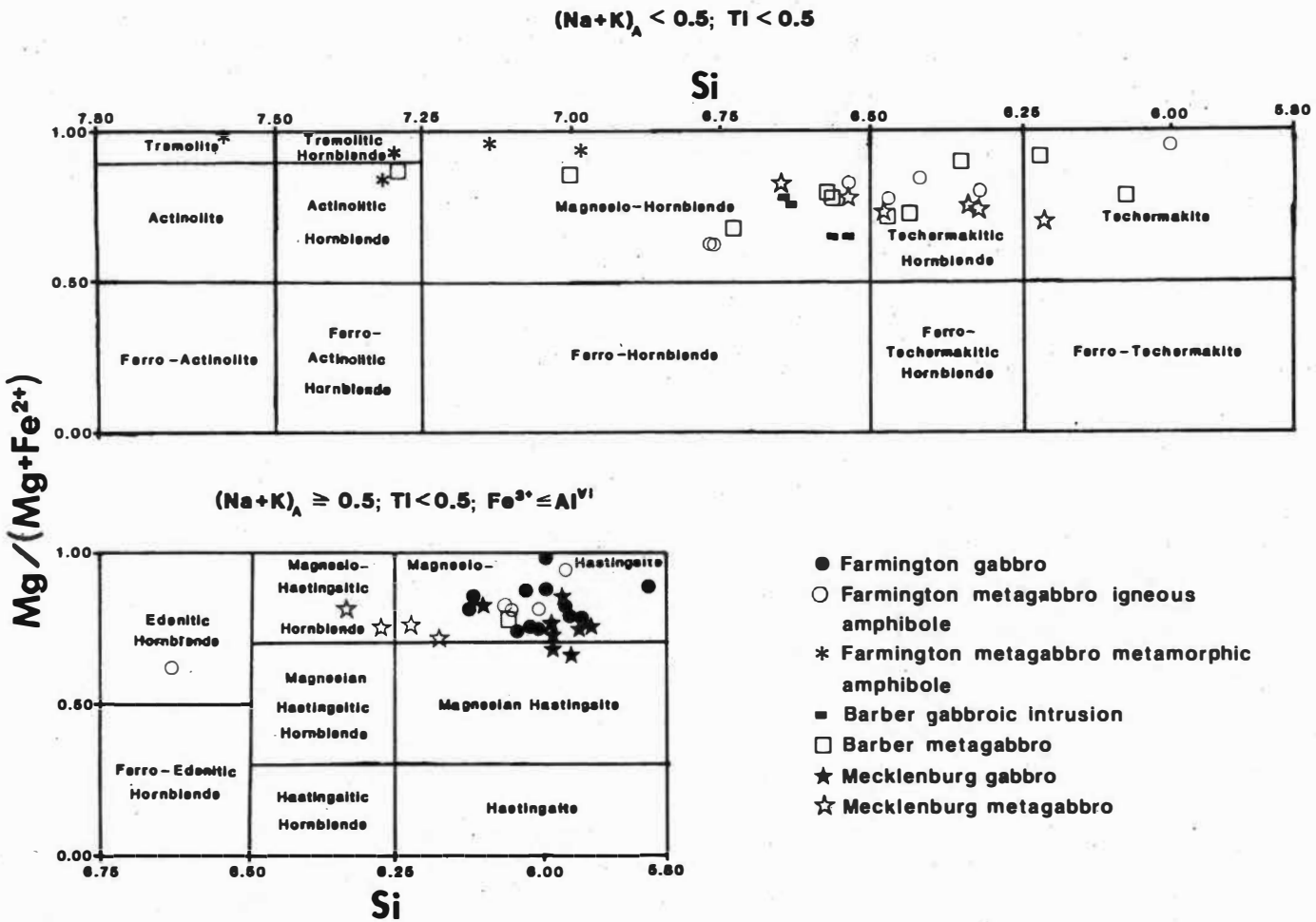

Figure 5. Calcic Amphibole Classification Diagram (from Leake, 1978). Plots of Farmington and Mecklenberg gabbro amphiboles overlap while Barber gabbro plots do not. Metagabbro amphiboles exhibit a considerable degree of overlap among all intrusions.

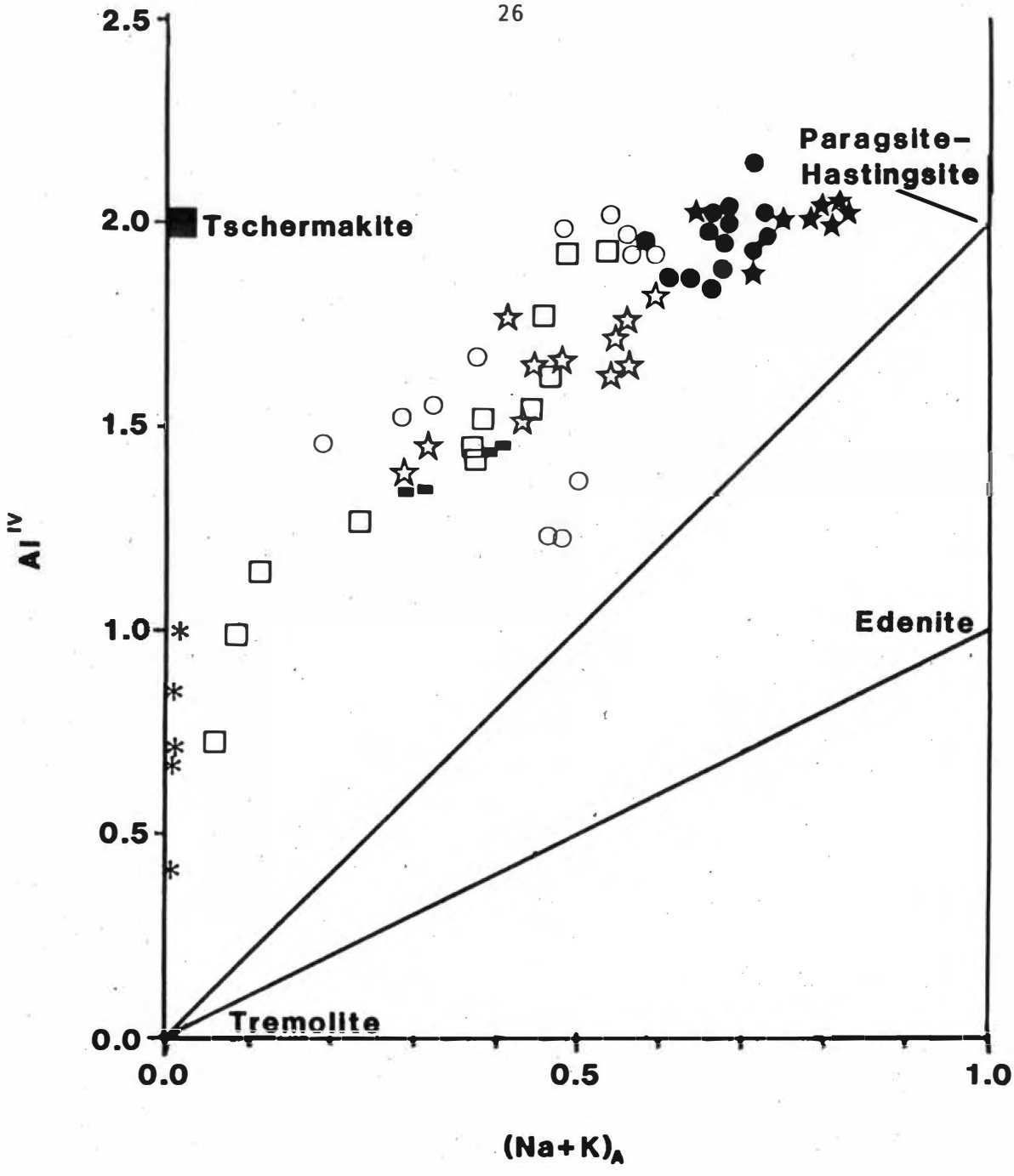

Figure 6. Plot of Al^{IV} Versus A-site Occupancy for Farmington, Barber, and Mecklenberg Ca-Amphiboles. Since plots are generally parallelling the paragasite-hastingsite-tremolite tie-line, a paragasite-hastingsite substitution is involved, but intercepts for the various plots fall between 0.4 and 1.4 indicating other substitutions involving Al(IV). Symbols are the same as in Figure 5, p. 25.

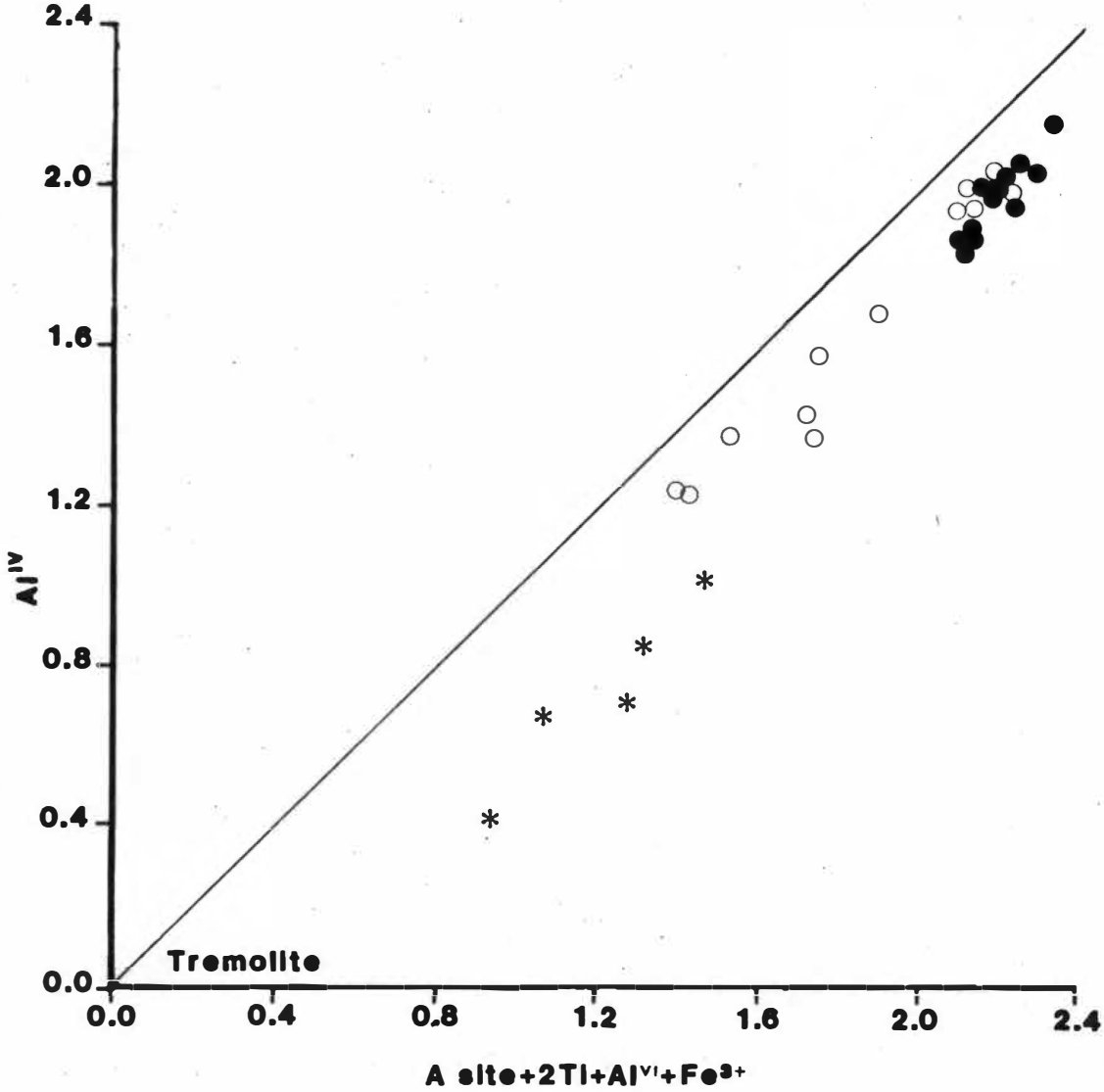

Figure 7. Plot Showing Variability of Al^{IV} Versus A-site + 2Ti + Al^{VI} + Fe^{3+}. Plots are for Farmington complex amphiboles only. Symbols are the same as in Figure 5, p. 25. Gabbro amphiboles and metagabbro igneous amphiboles plot parallel and close to the line (slope = 1.0) passing through the origin. This indicates that only a small substitution for Fe(3+), Al(VI), Ti, or A-site cations is involved. Metamorphic amphibole has an intercept of greater than 0.5 which indicates a much larger substitution possibly involving glaucophane.

Extra Al^{IV} can probably be accounted for by a minor gaucophane substitution. Amphibole comprises 1.6 to 21.8% of the gabbro excluding the fibrous amphibole (0-15%) from coronas.

Biotite flakes (0-0.9%) are found interstitial to plagioclase, as ragged flakes on hastingsite, and as rims on opaque minerals. Biotite is pleochroic from tan to reddish-brown. Electron microprobe analyses of biotite in two samples yielded FeO/(FeO + MgO) ratios of 0.27 and 0.23 (see Table A-2, Appendix).

Opaque minerals constitute 0.4 to 3.0% of the Farmington gabbro. Magnetite and ilmenite are the most abundant opaques with lesser amounts of pyrrhotite, pentlandite, pyrite, and hematite. Magnetite and ilmenite are found in symplectites (previously discussed), as interstitial grains, and as inclusions. Hercynitic spinel occurs at boundaries between magnetite and ilmenite. Sulfides are present as rounded bleds.

Apatite, sericite, chlorite, and serpentine are common accessory minerals. Euhedral to anhedral apatite is found as inclusions and interstitial to other grains. Veins and patches of sericite commonly alter plagioclase. Chlorite is found as an alteration of hornblende and pyroxene, and as a filling in veinlets. Serpentine forms as an alteration of olivine.

The International Union of Geological Sciences system of classification and nomenclature (Streckeisen, 1973) utilized a comparison of the modal percentages of the major minerals (plagioclase, orthopyroxene, clinopyroxene, amphibole, and olivine) to determine

petrologic classification and is used here to classify the rocks involved in this study. The plagioclase-orthopyroxene-clinopyroxene diagram (Figure 8a) shows that the Farmington gabbroic rocks are predominantly gabbronorites with some norites. On the basis of Figures 8b (amphibole-total pyroxene-olivine) and 8c (plagioclase-total pyroxene-amphibole), gabbronorites can be further subdivided into hornblende-olivine gabbronorites and hornblende gabbronorites, and norites can be subdivided into hornblende-olivine norites and hornblende norites.

Textures are generally hypidiomorphic granular to hypidomorphic inequigranular (Figure 9a). Early crystallization of plagioclase and olivine produced cumulate textures in which pyroxene and hornblende occur interstitially. In samples with abundant pyroxene and/or amphibole, poikilitic textures are formed enclosing cumulus plagioclase and olivine (Figure 9b). Oikocrysts of clinopyroxene and orthopyroxene crystallized from intercumulus liquid simultaneously along with the interstitial magnetite and ilmenite. In some instances, clinopyroxene occurs as discrete grains interstitial to plagioclase, enclosed in orthopyroxene oikocrysts, or partially rimmed by orthopyroxene. All occurrences of interstitial clinopyroxene are found in gabbronorites. The textural evidence suggests that the clinopyroxene crystallization preceded the crystallization of orthopyroxene and iron-titanium oxides in some cases. In most situations, clinopyroxene, orthopyroxene, and interstitial oxides coprecipitated. Amphibole oikocrysts formed from late magmatic intercumulus liquids through late-stage replacement of pyroxene, or as rims on opaques and pyroxenes by means of reaction

Figure 8. Petrologic Classification of Farmington Gabbro and Metagabbro Samples (from Strekeisen, 1973).

a. Plagioclase-orthopyroxene-clinopyroxene diagram showing distribution of norites (open circles), gabbronorites (open squares), and relict gabbronorites (stars).

b. Total pyroxene-olivine-amphibole diagram.

c. Plagioclase-total pyroxene-amphibole diagram. Metagabbro samples generally contain more amphibole and less plagioclase than the unmetamorphosed gabbro. Symbols same as above plus type I metagabbros are shown as filled squares, type II as filled circles, and type III as asterisks.

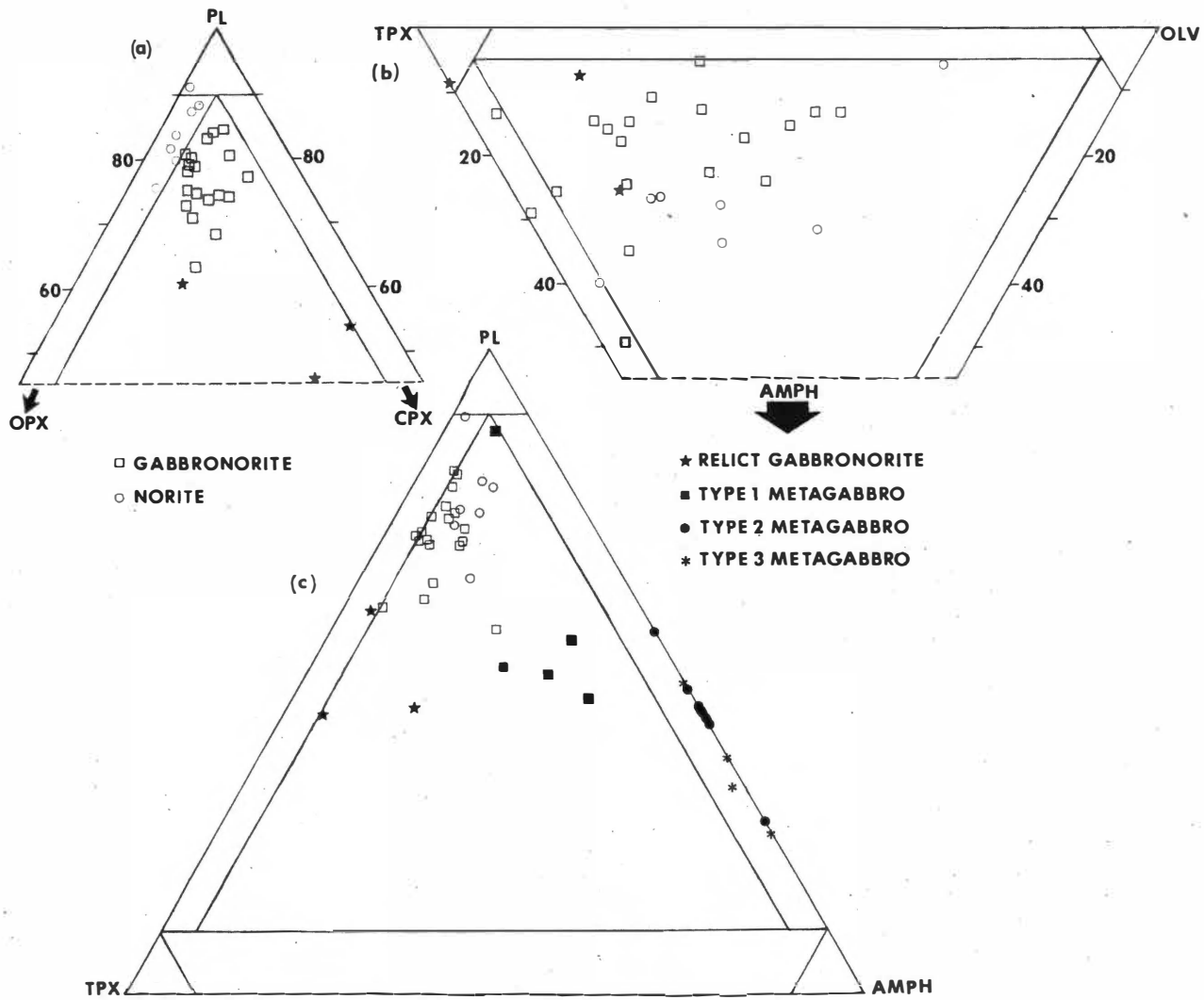
PL
(a)
80
80
60
60
OPX
CPX
TPX
OLV
(b)
20
20
40
40
AMPH
PL
(c)
TPX
AMPH
□ GABBRONORITE
○ NORITE
★ RELICT GABBRONORITE
■ TYPE 1 METAGABBRO
● TYPE 2 METAGABBRO
* TYPE 3 METAGABBRO

Figure 8.

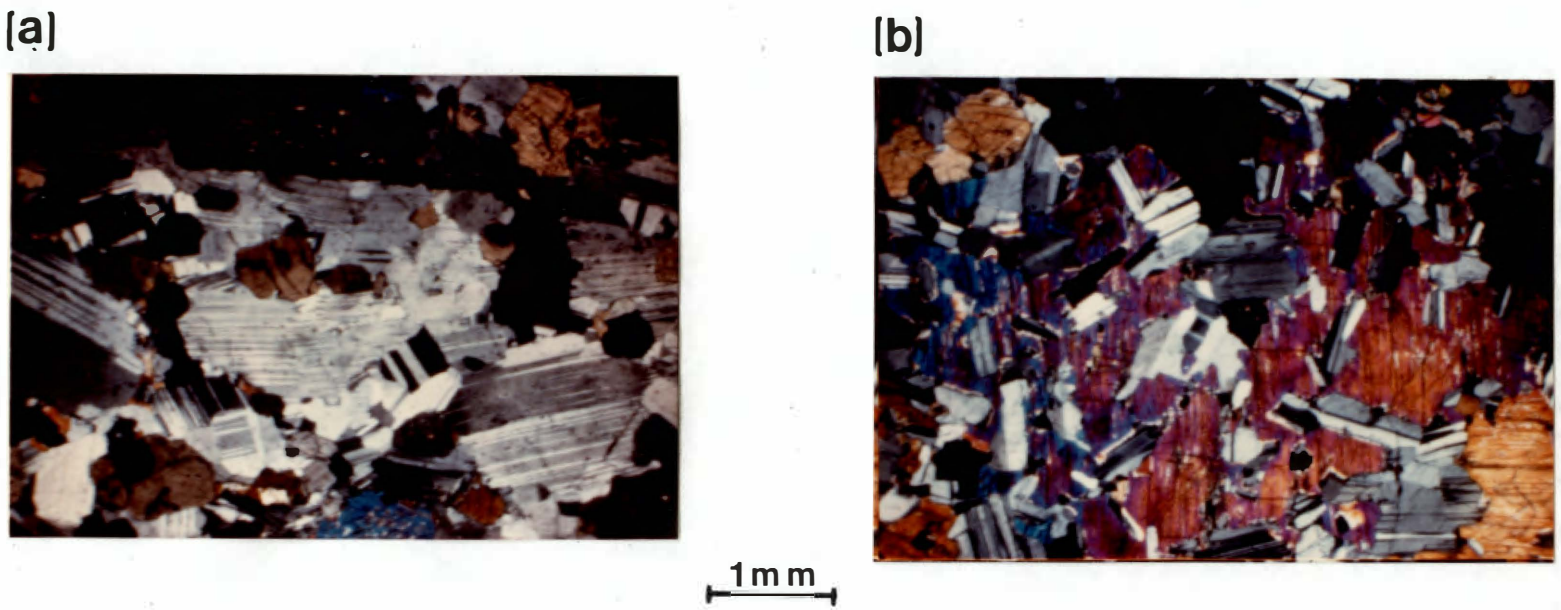

Figure 9. Photomicrographs of Farmington Gabbro.

a. Gabbronorite exhibiting a hypidiomorphic granular texture with subhedral plagioclase and pyroxene. Igneous foliation results from alignment of plagioclase and pyroxene (crossed nicols).

b. Poikilitic texture exhibited by clinopyroxene in a gabbronorite. Laths of plagioclase and grains of orthopyroxene and olivine are contained within the clinopyroxene oikocryst (crossed nicols).

with late-stage fluids. Biotite was produced by late-stage crystallization from the melt or replacement of pyroxene and amphibole and by reaction of late-stage fluids with opaques to form rims. Late-stage reaction of fluid between magnetite and ilmenite resulted in the production of hercynite. The alignment of plagioclase seen in many samples produces a foliation, but compositional layering was not observed. Restricted increases of FeO/(FeO + MgO) ratios in mafic silicates and lower anorthite contents indicates a limited range of progressive differentiation (Figure 4, p. 22).

Farmington Metagabbro

The Farmington metagabbro is composed of metamorphosed plutonic rocks with relict igneous features and can be subdivided into four types: metagabbro protolith, and metagabbro designated types I, II, and III. This classification is based on both texture and mineralogy. Modal percentages of minerals in metagabbro samples are presented in Table 7. Metagabbro protoliths have retained their original mineralogy and most of their original textures with some minor recrystallization (Figure 10a). This rock type contains plagioclase, orthopyroxene, clinopyroxene, amphibole, and, in some cases, olivine. Replacement of pyroxene by amphibole occurs in minor amounts as small patches within pyroxene and along cleavage traces. Metagabbro protoliths plot as olivine-hornblende gabbronorites for olivine-bearing samples and as gabbronorites for olivine-free samples (Figures 8a, 8b, and 8c). In type I metagabbro, the hypidiomorphic granular texture is preserved,

Table 7. Modal Variations: Farmington Metagabbro

	PLG	AMP	CPX	OPX	QTZ	OLV	BIO	APA	OPA	HEM	CHL	EPI	SERC	SERP	TTN
3-15-3	53.2	32.0	11.6	-	-	-	-	-	0.4	-	2.5	0.2	0.1	-	-
3-15-10	45.3	48.7	-	-	-	-	T	-	T	T	4.1	1.7	0.2	-	T
4-5-10A	42.8	56.0	-	-	-	-	-	T	T	0.1	0.3	0.9	T	-	-
4-20-17	40.4	57.3	-	-	-	-	0.3	0.2	0.5	0.4	0.6	0.3	-	-	-
4-21-5	28.2	61.1	1.6	-	-	-	0.1	0.1	3.8	-	0.1	3.5	1.5	-	-
5-10-5	35.6	61.2	-	-	0.5	-	-	-	2.3	0.4	-	-	T	-	-
6-13-1	40.9	58.1	-	-	0.4	-	-	0.4	-	T	-	0.2	-	-	-
6-13-4	37.5	48.4	-	-	-	-	0.2	-	6.7	0.9	0.2	4.2	1.9	-	-
6-13-14	24.3	72.2	-	-	-	-	-	-	0.1	-	0.3	3.1	0.1	-	-
6-14-2	44.0	55.4	-	-	-	-	T	T	0.1	T	-	0.5	T	-	T
6-14-11	24.4	67.9	-	-	1.4	-	-	-	5.3	0.1	-	0.5	0.4	-	-
6-15-1	46.1	52.6	-	-	0.8	-	-	-	0.1	0.2	0.1	0.2	-	-	-
6-15-6	23.8	67.9	-	-	2.6	-	-	1.0	3.5	0.1	-	1.1	T	-	-
8-4-3	41.6	35.8	13.2	-	-	-	0.1	0.4	8.9	-	-	-	-	-	-
8-4-4	38.1	4.7	33.1	12.1	-	10.7	T	T	1.1	-	-	-	T	0.2	-
8-4-5	40.2	14.7	29.4	4.8	-	8.2	-	-	1.6	-	0.4	-	0.1	0.6	-
8-4-11	49.0	25.7	22.5	-	-	-	T	0.5	1.8	-	0.4	0	0.1	-	-
9-6Q-5A	54.1	41.5	0.1	-	-	-	-	T	0.4	0.1	-	-	1.2	-	-
9-6Q-7A	65.4	5.2	4.0	-	7.6	-	13.5	0.6	3.2	-	T	-	0.2	-	0.3
9-6Q-7C	58.4	3.6	13.0	23.5	-	-	0.1	0.1	1.0	-	0.1	-	0.3	-	-
9-7-1A	46.6	30.8	16.8	-	-	-	0.5	T	5.3	-	-	-	-	-	-

Figure 10. Photomicrographs of Farmington Metagabbro.

a. Metagabbro protolith containing olivine. Olivine shows distinct corona development with an inner rim of orthopyroxene around olivine grains and an outer rim of amphibole and spinel in contact with plagioclase (crossed nicols).

b. Type I metagabbro containing a hornblende oikocryst. The oikocryst surrounds an olivine pseudomorph as well as grains of pyroxene and plagioclase (plane polarized light).

c. Relict igneous amphibole in a type II metagabbro. Small clinopyroxene relicts are found poikiliticly enclosed in the altered igneous amphibole (dark brown to greenish brown). Green metamorphic amphibole grains are pseudomorphs after pyroxene (plane polarized light).

d. A type III metagabbro that exhibits banding. Plagioclase, amphibole, and epidote are present (crossed nicols).

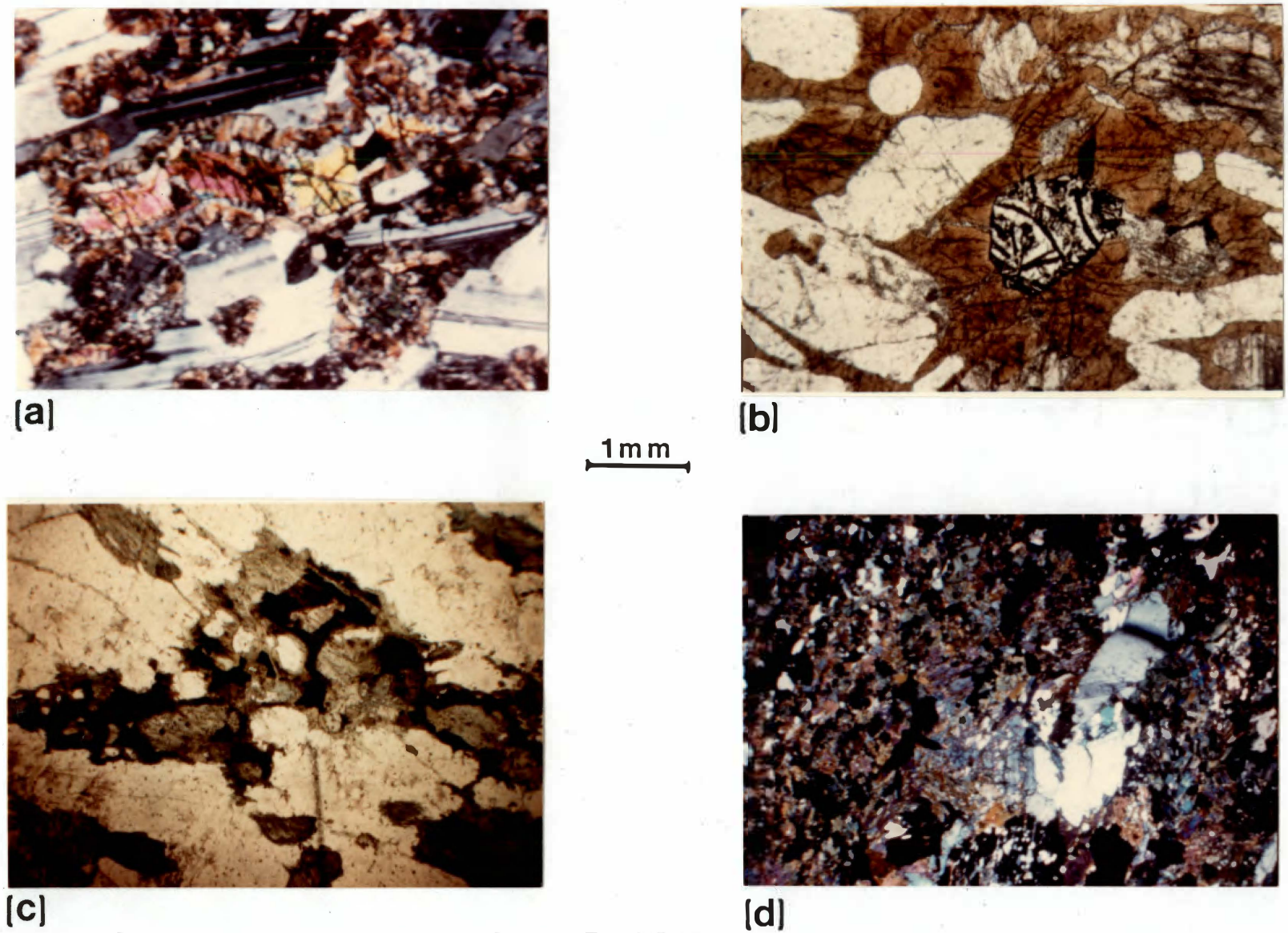

Figure 10.

but increased metamorphic alteration has eliminated olivine and orthopyroxene. Serpentine pseudomorphs ± opaques after olivine and altered symplectite are present along with clinopyroxene and igneous amphibole. Metamorphic amphibole extensively replaces some clinopyroxenes (Figure 10b). Type I metagabbros are shown plotted on the plagioclase-pyroxene-amphibole diagram in Figure 9c.

Type II and III metagabbros are dominated by amphibole and plagioclase (Figure 8c) with little or no clinopyroxene occurring and may have considerable amounts of epidote. Igneous amphibole oikocrysts are usually preserved in type II metagabbro and may show only slight to moderate alteration, but metamorphic amphibole predominates (Figure 10c). Type II rocks may or may not show foliation. Type III metagabbro is similar to type II in mineralogy, but igneous amphibole is sometimes strongly altered or altogether absent. Compositional and textural banding distinguishes type III from type II (Figure 10d). These bands are usually discontinuous. Textural banding takes the form of fine-grained "salt and pepper" texture alternating with coarser-grained granoblastic bands. Samples transitional between types II and III contain both well preserved igneous amphibole and banding. Widely varying amounts of biotite, quartz, and opaques (magnetite, ilmenite, hematite, and sulfides) occur along with other accessory minerals such as apatite, chlorite, hercynite, serpentine, sericite, titanite, and zircon. The above system of metagabbro classification is very similar to that use by Hermes (1968) and is not unlike that employed by Clark (1980), but differs from Clark's in that his was based mostly on mineralogy.

Plagioclase (23.8 to 65.4%) forms fine- to coarse-grained subhedral crystals. The grains are generally faintly zoned, but one case of strong normal zoning occurs (An_{18} - An_{40}) in a type I metagabbro. Anorthite content for all metagabbros ranges from An_{18} to An_{93}. In the olivine-bearing metagabbro protolith, the anorthite content is found to be higher (An_{82} - An_{93}) than in metagabbro protolith where olivine is absent (An_{58} - $An_{66.5}$). Type I metagabbro analyses range from An_{18} to An_{61} and the Type II metagabbro exhibits an anorthite content of An_{54} to An_{57}. Inclusions of opaques and other minerals are less abundant than in the plagioclase of the unmetamorphosed gabbro.

Amphibole accounts 3.6 to 72.2% of the metagabbroic rocks. Two groups of amphiboles are present in metagabbros: igneous amphiboles and metamorphic amphiboles. Igneous amphiboles form large oikocrysts containing pyroxene, plagioclase, and olivine pseudomorphs and as rims on pyroxene and opaques that are pleochroic from light brown to reddish-brown or dark brown. Igneous amphibole can be represented on the pyroxene quadrilateral in Figure 4 (p. 22) in terms of Mg, Fe, and Ca components. Igneous amphibole compositions show two groupings based on the classification of Leake (1978) in Figure 5 (p. 25). The second group plots in the field of magnesio-hastingsite and appears similar to unmetamorphosed gabbroic amphibole, but tends to be more tschermakitic (Figure 5 and Figure 6, p. 26). Variability in A-site occupancy and Al^{IV} are primarily accounted for by the paragasite-hastingsite substitution.

Metamorphic amphibole is anhedral and pleochroic from pale bluish-green or pale green to green or brownish-green. Grains generally have a fibrous habit and are frequently poikilitic containing grains of quartz and pyroxene relicts. The metamorphic amphibole replaces or forms pseudomorphs of pyroxene and occurs as an alteration of igneous amphibole. Amphibole formed from alteration of pyroxene shows a compositional range from tremolite to tremolitic hornblende or actinolitic hornblende field like its unaltered igneous precursor but shows a considerable increase in Si and, generally, a slight increase in the $Mg/(Mg + Fe^{2+})$ ratio (Figure 5, p. 25). The paragasite-hastingsite substitution does not account for all of the variability seen in metamorphic amphiboles (Figures 6 and 7, pp. 26 and 27). A glaucophane substitution may be involved where Al^{VI} is compensated by Mg^{VI}.

Orthopyroxene (0-23.5%) has a compositional range of $Wo_2En_{77}Fs_{21}$ to $Wo_2En_{68}Fs_{30}$ and forms discrete medium to coarse subhedral crystals interstial to plagioclase and poikilitic grains. Fine exsolution lamellae of clinopyroxene are present as well as exsolved plates of reddish-brown spinel. Orthopyroxene was only found in relict gabbro.

Clinopyroxene (0-33.1%) is found as subhedral, medium to coarse grains and may be poikiliticly enclosed in igneous amphibole or orthopyroxene and as clinopyroxene relicts present in metamorphic amphibole. Exsolution of orthopyroxene parallel to (100) and opaques parallel to (010) are common. Clinopyroxene compositions range from $Wo_{43}En_{46}Fs_{11}$ to $Wo_{44}En_{41}Fs_{15}$.

Olivine is present in metagabbro protoliths only. Anhedral olivine grains have well developed coronas. These double coronas between plagioclase and olivine have an outer rim of radially fibrous amphibole with intergrowths of vermicular spinel and an inner rim of radially prismatic orthopyroxene much like the coronas seen in the Farmington gabbro. Unlike the postmetamorphic gabbro, the development of coronas in the premetamorphic gabbro appears unrelated to fractures or veins and could be a result of regional metamorphism. Average composition for the single occurrence of olivine in relict gabbro is Fo_{82}.

Epidote (0-4.2%) occurs as anhedral to euhedral grains in veinlets, as prisms, and columnar crystals and aggregates replacing plagioclase. The epidote may replace plagioclase along particular zones within the grain or as rims between plagioclase and amphibole.

Light greenish-brown to dark brown tabular flakes of biotite (0-13.5%) are found as reaction rims along with amphibole, and interstitially to plagioclase. In type II metagabbro it is found altering to chlorite. Inclusions of zircon, quartz grains, and opaques are common in biotite. A FeO/(MgO + FeO) ratio of 0.44 was determined in one sample (see Table A-2, Appendix).

Quartz (0-7.6%) is present as anhedral interstial grains, as grains in biotite, and included in amphibole pseudomorphs of pyroxene. The occurrence of quartz in amphibole pseudomorphs is probably the result of pyroxene and plagioclase reacting to form amphibole with small amounts of silica left over from the reaction.

Opaque minerals (0-7.4%) found are magnetite, ilmenite, pyrite, pyrrhotite, and hematite. They form interstitial grains, inclusions, intergrowths, and precipitates from exsolution. Magnetite-ilmenite symplectite forms along olivine grain boundaries with orthopyroxene (previously discussed) in metagabbro protolith and with amphibole pseudomorphs of orthopyroxene bordering olivine pseudomorphs in type I metagabbro. Hematite occurs as discrete grains or as oxidation or exsolution lamellae in ilmenite. Exsolved magnetite and ilmenite are common in pyroxenes and less common in amphibole. An opaque dust is found in some amphiboles of type II and III metagabbros.

Accessory minerals such as apatite, chlorite, sericite, serpentine, titanite, hercynitic spinel, and zircon are present in minor amounts. Apatite occurs as inclusions in mafic minerals and plagioclase and as interstial grains. Chlorite forms pseudomorphs after biotite and pyroxene, as veinlets and as irregular patches. Sericite forms veinlets and fibrous masses replacing plagioclase. Anhedral hercynitic spinel occurs with magnetite and ilmenite interstitial to mafic grains. Serpentine forms greenish yellow pseudomorphs of olivine or masses replacing olivine. Titanite rims hematite and opaques in some type II and III metagabbros and forms small prisms. Inclusions of zircon in biotite are subhedral to euhedral.

Igneous textures vary depending on the presence or absence of olivine. In olivine-bearing rocks, textures are hypidiomorphic granular to hypidiomorphic inequigranular. Poikilitic textures occur, but are not common. The alignment of plagioclase denoting layering is

rare. Plagioclase, olivine, and clinopyroxene appear to be the cumulus phases. The early crystallization of plagioclase, olivine, and clinopyroxene was followed by the crystallization of rare orthopyroxene oikocrysts from intercumulus liquid. Opaques crystallized along with orthopyroxene forming interstial grains. Amphibole crystallized from a late-stage liquid to form oikocrysts and rims on mafic and opaque grains or formed as late-stage replacement of mafic grains.

Olivine-free metagabbro protoliths show hypidiomorphic granular to hypidiomorphic inequigranular textures like olivine-bearing rocks, but poikilitic textures are rare and igneous layering is very common with plagioclase being moderately to strongly aligned. Plagioclase, orthopyroxene, and clinopyroxene crystallized early from the magma and may have settled. Minor amounts of intercumulus material formed interstial opaques and rare, web-like amphibole oikocrysts during late magmatic crystallization. This process produced mesocumulate gabbronorites. Continued crystal settling resulted in a more siliceous magma as seen in some type I metagabbro. These type I rocks showed early crystallization of plagioclase and pyroxene. Continued plagioclase growth resulted in strong normal zoning. Late-stage crystallization produced amphibole rims on pyroxene, interstitial anhedral quartz, and biotite jacketing mafic grains. Biotite forms slightly poikilitic grains as well. The close proximity of the above two rock types implies that crystallization has been affected by crystal settling of early formed phases which resulted in igneous layering.

Areal Variations

The Farmington complex exhibits limited petrologic areal variations and generally lacks systematic variations in modal mineralogy (Figure 11). The norites of the Farmington gabbroic intrusion all occur across the central portion of the northern half of the pluton. Gabbronorites are found over the remaining exposed area of the pluton. The absence of systematic areal variation in modal mineralogy may be the result of insufficient sampling or exposure. Another possibility is that the Farmington complex may have been only recently unroofed.

The Farmington metamorphosed gabbroic rocks are predominantly type II and III metagabbro. Type I metagabbro and relict gabbronorites occur locally, but almost all are situated in the southern part of the metagabbroic intrusion. It is not unusual for more than one type to occur in a single outcrop. The lack of systematic variations in the metagabbro is likely due to the variation in local water content (Hermes, 1968) and the metagabbro being comprised of more than one intrusion.

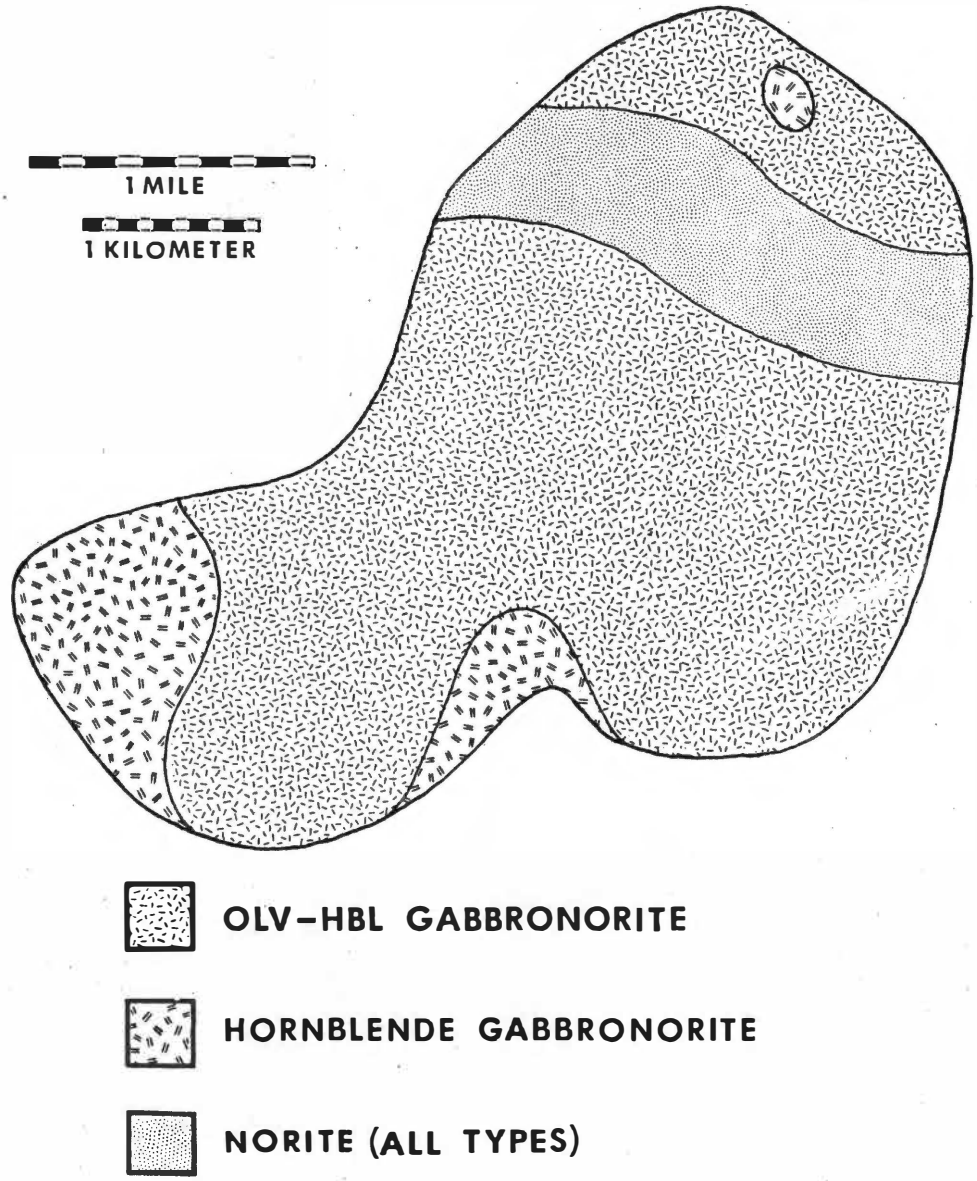

Figure 11. Petrologic Areal Variations for the Farmington Gabbroic Intrusion. A band of norite occurs across the north central portion of the pluton while hornblende gabbronorite and olivine-hornblende gabbronorite cover the remaining area.

V. PETROGENESIS

Emplacement as Multiple Intrusions

The Farmington complex consists of at least two and possibly more intrusions. It does not appear to have been emplaced as a single gabbroic intrusion which underwent metamorphism and retained an unaltered core. The unaltered gabbroic rock is a separate pluton intruding the metagabbro. Xenoliths or roof pendants of metagabbro have been found in the gabbroic pluton (previously cited in Section III--Field Relations). A more intense positive gravity anomaly over the gabbroic pluton would also suggest that it represents a separate body extending deeper than the surrounding metagabbro. In addition, the lack of alteration and recrystallization of the gabbroic pluton is the most distinguishing characteristic that sets it apart from the metagabbro.

The Farmington metagabbro itself also represents more than one intrusion. Xenoliths of older metagabbro within the main body of metagabbro were found, indicating the presence of at least two generations of metagabbro. The existence of two different relict gabbronorites, one of which is olivine-bearing and the other which is not, and two distinct groups of igneous amphiboles may also indicate two separate intrusions.

Metamorphism

As mentioned above, the metamorphosed gabbroic rocks show varying degrees of metamorphism ranging from greenschist to

greenschist-lower amphibolite transitional grade. This appears lower than regional metamorphic grade, which is middle to upper amphibolite grade northeast of the study area in the Charlotte belt (Espenshade et al., 1975).

The variable nature of the metamorphism is reflected in the modal percentages and effects on primary minerals. Limited metamorphism resulted in some amount of recrystallization and alteration of anhydrous mafic minerals along fractures, cleavage traces, and, in some cases, along grain boundaries to minor amounts of hydrous phases. More highly developed metamorphism eliminated olivine and orthopyroxene from the mineral assemblage, and only chlorite, tremolitic amphibole, or serpentine pseudomorphs remain. Clinopyroxene is the last anhydrous mafic silicate to disappear, forming tremolitic or actinolitic hornblende. Igneous amphibole is frequently preserved, but in some cases it is also altered and recrystallized. Plagioclase becomes more sodic, less zoned, and tends to form epidote in rocks that have approached equilibrium with the prevailing P-T conditions. Progressive metamorphism of igneous amphibole resulted in a decrease of A-site occupancy, Al^{IV}, and Ti and an increase in Si. This same trend of metamorphic alteration of amphibole is seen in metagabbroic rocks of the Central Bohemian Pluton, Czechoslovakia (Vejnar, 1975) and in the metagabbro-amphibolite sequence of Hidaka, Japan (Grapes et al., 1977).

The observed variability in the metagabbro could be due to the localized availability of H_2O during regional metamorphism and its irregular distribution resulting from localized shearing (Hermes, 1968).

Another possibility is the repeated intrusion of gabbro into earlier gabbros, introducing heat and water (McSween, 1981; McSween et al., 1984). Distance from the latest intrusion and shears acting to localize fluids would then bring about the variable nature of metamorphism and account for lower than regional grade effects.

Comparison with Other Mafic Complexes

Many similarities and differences exist between the Farmington complex and other mafic complexes in the Charlotte belt. The Barber complex (Clark, 1980; McSween et al., 1984) and the Mecklenburg complex (Hermes, 1969, 1970) lying south of the study area in North Carolina (Figure 1, p. 2) represent two such bodies.

The most striking difference between the Barber complex and the Farmington complex is that the unmetamorphosed gabbroic pluton in the former is a norite containing quartz and no olivine, unlike the Farmington gabbro. Mineral isochrons also indicate that the Barber gabbroic pluton is older (479 ± 24 my) than the Farmington pluton (399 ± 27 my) (McSween et al., 1984). Despite the differences between the Barber and Farmington unmetamorphosed intrusions, the metagabbro in these complexes show several similarities. The metagabbroic rocks from both complexes contain relict olivine-bearing gabbronorites and olivine pseudomorphs. The modal mineralogies in the two metagabbro bodies are both dominated by amphibole and plagioclase. The compositions of amphiboles in the Barber and Farmington metagabbros are nearly identical in terms of end members (Figures 5, 6, and 7,

pp. 25, 26, and 27). In addition, hornblendite is associated with both bodies. The main difference between the Barber metagabbro and Farmington metagabbro is in the average anorthite content of plagioclase, which shows a wider range in the Farmington metagabbro (An_{84} - An_{28}) than the Barber metagabbro (An_{93} - An_{74}).

The Mecklenburg gabbro exhibits some similarities with the Farmington gabbroic intrusion. The anorthite contents for plagioclase are nearly identical in the two intrusions: An_{68} - An_{50} for the Farmington plagioclase versus An_{67} - An_{51} for the Mecklenburg plagioclase. Amphiboles are magnesio-hastingsites in both intrusions and show similar substitution trends (Figures 5, 6, and 7). Differences between the two unmetamorphosed bodies are exemplified by a greater variation in modal percentages of major minerals and higher FeO/(FeO + MgO) ratios of ferromagnesium minerals in the Mecklenburg gabbro. Several differences exist between the Farmington and Mecklenburg metagabbros. The Mecklenburg metamorphosed intrusion lacks the relict gabbronorites seen in the Farmington metagabbro. Olivine pseudomorphs are not found in the Type I metagabbro of the Mecklenburg complex and more pyroxene occurs in the mode for the Mecklenburg metagabbro, which may be a result of less metamorphic alteration. The anorthite content for plagioclase is more restricted in the Mecklenburg metagabbro (An_{62} - An_{38}) than in the Farmington metagabbro. In addition, there is no mention of hornblendites being associated with the Mecklenburg metamorphosed intrusion. The Farmington metagabbro shows a similarity to the Mecklenburg

metagabbro in the compositional range of its clinopyroxenes. Igneous amphiboles are also very similar, in that both metagabbro bodies contain two distinct groups of amphiboles (Figure 5, p. 25) and show similar substitution trends (Figures 6 and 7, pp. 26 and 27).

Tectonic Setting

The similarity of the Farmington complex and other bodies in the same linear chain and their generally regular spacing have suggested to some workers that these bodies formed over an active subduction zone (Clark, 1980; McSween et al., 1984) and that the gabbro-metagabbro association is not a fortuitous one (McSween, 1981a). The other complexes show calc-alkaline basalt and low-K tholeiite affinities and suggest an origin in a continental margin subduction zone (Clark, 1980; McSween, 1980). The existing similarities and areal relationship of the Farmington complex with the complexes to the southwest would indicate that the Farmington complex has the same origin.

McSween (1981a) has suggested that these complexes represent "chimneys" formed by repeated intrusion of magma into the same conduits, as indicated by geophysical models of magma ascent in subduction zones (Marsh, 1976; 1978). This process would heat the lithosphere sufficiently to insulate successive magma bodies and allow them to move to higher levels. The metagabbro protolith from the Farmington complex differs mineralogically and in modal percentages of minerals from the unmetamorphosed gabbro, suggesting that material was possibly vented to higher levels from the later magma pulse. The

lack of a contact metamorphic aureole would suggest that the metagabbros were hot and that the irregularity of metamorphism is a result of fluids introduced by repeated intrusion. Therefore, the multiple intrusive nature of the Farmington complex may support the previously proposed tectonic setting and model of emplacement for metagabbro-gabbro complexes.

LIST OF REFERENCES

LIST OF REFERENCES

Albee, A. L., and Ray, L., 1970, Correction of electron probe microanalysis of silicates, oxides, carbonates, phosphates, and sulfate: Analyt. Chem., v. 42, pp. 1408-1414.

Ambler, E. P., and Ashley, P. M., 1977, Vermicular orthopyroxene-magnetite symplectites from the Wateranga layered mafic intrusion, Queensland, Australia: Litho, v. 10, pp. 163-172.

Ambler, E. P., and Ashley, P. M., 1980, Mineralogy and petrology of the Dutchman's Creek gabbroic intrusion, South Carolina: discussion: Am. Mineral., v. 65, pp. 1302-1303.

Bence, A. E., and Albee, L. A., 1968, Empirical correction factors of the electron microanalysis of silicates and oxides: Jour. of Geol., v. 76, pp. 382-403.

Butler, J. R., 1965, Gabbro plutons in the Carolina Piedmont (abstr.): Geol. Soc. of Am. Special Paper No. 82, p. 294.

Butler, J. R., 1966, Geology and Mineral resources of York County, South Carolina: South Carolina State Devel. Board, Bull. 33.

Bulter, J. R., 1978, Geologic map of Charlotte 1° x 2° NTMS area, N. C. and S. C.: from Heffner, G. D., and Ferguson, R. B., Savannah River Laboratory hydrogeochemical stream sediment reconnaissance preliminary raw data release Charlotte 1° x 2° NTMS area, N. C. and S. C., National Uranium Resource Eval. Prog., Dept. of Energy, GJBX-40(78), DPST-78-146-1: E. I. Dupont, De Nemours, and Co., Savannah River Laboratory, Aiken, S. C.

Bulter, J. R., and Fullagar, P. D., 1978, Petrochemical and geochronological studies of plutonic rocks in the Southern Appalachians: III. Leucocratic adamellites of the Charlotte belt near Salisbury, N. C.: Geol. Soc. of Am. Bull., v. 89, pp. 460-466.

Butler, J. R., and Ragland, P. C., 1969, A petrochemical survey of plutonic intrusions in the Piedmont, Southeastern Appalachians, U.S.A.: Contr. to Mineral. and Petrol., v. 24, pp. 164-190.

Cabaup, J. J., 1969, Origin and differentiation of the gabbro in the Concord ring dike, Cabarrus County, North Carolina Piedmont: Unpublished M.S. thesis, Univ. of North Carolina at Chapel Hill, 42 p.

Chalcraft, R. G., 1970, Petrography and geophysics of the Rock Hill gabbro Pluton, York County, S. C.: Southeastern Geology, v. 11, pp. 153-171.

Chalcraft, R. G., Lawerence, D. P., Taylor, C. A., Jr., Snoke, A. W., 1978, The petrology of the Greenwood pluton, Greenwood County, S. C.: South Carolina Geol. Surv., pp. 40-46.

Chayes, F., 1956, Petrographic modal analysis: John Wiley and Sons, Inc., New York, N.Y., 113 p.

Clark, S. F., 1979, Petrology of the Bear Poplar and Barber mafic intrusions, North Carolina: Unpublished M.S. thesis, Univ. of Tennessee, Knoxville, 76 p.

Constantine-Herrera, S. E., 1971, Geology of the Cleveland gabbro, Rowan County, North Carolina: Unpublished M.S. thesis, Univ. of North Carolina at Chapel Hill.

Deetz, S. F., 1979, Mineralogy and petrology of the Chester pluton: Unpublished M.S. thesis, Univ. of Tennessee, Knoxville, 55 p.

Esbensen, K. H., 1978, Coronites from the Fongen gabbro complex, Trondheim region, Norway: Role of water in the olivine-plagioclase reaction: Neues Jahrbuch fur Mineral. Abhandlugen, v. 132, pp. 113-135.

Espenshade, G. H., Rankin, D. W., Shaw, K. W., and Neuman, R. B., 1980, Geologic map of the east half of the Winston-Salem quadrangle N. C.-Va., Map I-709-B: Miscellaneous Investigation Series, U.S.G.S.

Fleet, M. E., Bilcox, G. E., and Barnet, R. L., 1980, Oriented magnetite inclusions in pyroxenes from the Greenville province: Canadian Mineralogist, v. 18, pp. 89-99.

Fullagar, P. D., 1971, Age and origin of plutonic intrusions in the Piedmont of the Southeastern Appalachians: Geol. Soc. of Am. Bull., v. 82, pp. 2845-2862.

Garrison, J. R., Jr., and Taylor, L. A., 1981, Petrogenesis of pyroxene-oxide intergrowths from kimberlite and cumulate rocks: co-precipitation or exsolution?: Am. Mineral., v. 55, pp. 723-740.

Glover, L. III, and Sinha, A. K., 1973, The Virgilina deformation, a late Precambrian (?) orogenic event in the central Piedmont of Virginia and North Carolina: Am. Jour. of Science, Cooper volume 273-A, pp. 234-251.

Grapes, R. H., Hashimoto, S., and Miyashita, S., 1977, Amphiboles of a metagabbro-amphibolite sequence, Hidaka metamorphic belt, Hokkaido: Jour. of Petrol., v. 18, part 2, pp. 285-318.

Hadley, J. B., 1973, Igneous rocks of the Oxford area, Granville, N. C.: Am. Jour. of Science, v. 273-A, pp. 217-233.

Hermes, O. D., 1968, Petrology of the Mecklenburg gabbro-metagabbro complex, North Carolina: Contr. to Mineral. and Petrol., v. 18, pp. 270-294.

Hermes, O. D., 1970, Petrochemistry of coexistent mafic silicates from the Mecklenburg gabbro-metagabbro complex, North Carolina: Geol. Soc. of Am. Bull., v. 81, pp. 137-163.

Jurney, R. C., and Bacon, S. R., 1927, Soil survey of Davie county, North Carolina: Bureau of Chemistry and Soils, U.S. Dept. of Agriculture, series 1927, no. 5, 26 p.

Leake, B. E., 1978, Nomenclature of amphiboles: Am. Mineralogist, v. 63, pp. 1023-1052.

Marsh, B. D., 1976, Some Alention andesites: their nature and sources: Jour. Geol., v. 84, pp. 27-45.

Marsh, B. D., 1978, On the cooling of ascending andesitic magma: Phil. Trans. Royal Soc. London, v. 288, pp. 611-625.

Mathews, V., III, 1969, The Gladesville norite and its relationship to similar mafic plutons in the Georgia Piedmont (abstr.): Geol. Soc. Am. Abstracts with Programs, v. 4, no. 50.

McCauley, J. R., 1971, Relationship between the Carolina Slate belt and the Charlotte belt in Newbury Co., S. C.: South Carolina State Devel. Board, Geol. Notes, v. 5, pp. 59-71.

McSween, H. Y., Jr., 1970, Petrology of Charlotte and Kings Mountain belt rocks in northern Greenwood County, S. C.: South Carolina Devel. Board, Geol. Notes, v. 14, pp. 57-84.

McSween, H. Y., Jr., 1980, Mineralogy and petrology of the Dutchman's Creek gabbroic intrusion, South Carolina: reply: Am. Mineralogist, v. 65, pp. 1304-1305.

McSween, H. Y., Jr., 1981a, Gabbro-metagabbro complexes: a mechanism for magma ascent?: Geol. Soc. Am. Abstracts with Programs, v. 13, p. 508.

McSween, H. Y., Jr., 1981b, Petrology of the Ogden gabbroic intrusion, York county, S. C.: South Carolina Geol., v. 25, pp. 9-100.

McSween, H. Y., Jr., and Nystrom, P. G., Jr., 1979, Mineralogy and petrology of the Dutchman's Creek gabbroic intrusion, South Carolina: Am. Mineralogist, v. 64, pp. 531-545.

McSween, H. Y., Jr., Sando, T. W., Clark, S. R., Harden, J. T., and Strange, E. A., 1984, The gabbro-metagabbro association of the southern Appalachian Piedmont: Am. Jour. of Science, v. 284, pp. 437-461.

Medlin, J. H., 1969a, Comparative petrology of two igneous complexes in the South Carolina Piedmont: Unpublished Ph.D. dissertation, Pennsylvania State Univ.

Medlin, J. H., 1969b, Petrology of two mafic igneous complexes in South Carolina Piedmont (Abstr.): Geol. Soc. Am. Abstracts with Programs, v. 4, no. 52.

Medlin, J. H., Thorton, C. P., and Gold, D. P., 1972, Petrology of the mafic igneous complexes in southeastern U.S. Piedmont; II. The Buffalo mafic igneous, Union County, S. C.: Southeastern Geol., v. 14, pp. 73-106.

Melton, D., 1980, Personal communication.

Morgan, B. A., 1963, A gravity survey of a ring-dike near Concord, N. C.: Unpublished M.S. thesis, Univ. North Carolina at Chapel Hill.

Murthy, M. V. N., 1958, Coronites from India and their bearing on the origin of coronas: Geol. Soc. Am. Bull., v. 69, pp. 23-28.

Myers, C. W., 1968, Geology of the Presley Mill gabbro, Putnam County, Ga.,: Unpublished M.S. thesis, Univ. of Georgia.

Neilson, M. J., and Brockman, G. F., 1977, The error associated with point counting: Am. Mineralogist, v. 62, pp. 1238-1244.

Olsen, B. A., 1982, Petrogenesis of the Concord gabbro-syenite complex, Cabarrus County, N. C.: Unpublished M.S. thesis, Univ. of Tennessee-Knoxville, 72 p.

Ragland, P. C., Rogers, J. J. W., and Justus, 1968, Origin and differentiation of Triassic dolerite magmas, North Carolina, U.S.A.: Contr. Mineral. and Petrol., v. 20, pp. 57-80.

Starmer, I. C., 1969, Basic plutonic intrusions of the Risor-Sondeled area, Norway: The original lithologies and their metamorphism: Norsk. Geol. Tidsk., v. 49, pp. 403-431.

Streckeisen, A. L., 1973, Plutonic rocks--classification and nomenclature: Geotimes, v. 18, pp. 43-63.

Taylor, C. A., Jr., and Butler, J. R., 1982, Geology and gravity of the northern end of the Charlotte belt, and Davie County Mesozoic basin, central North Carolina Piedmont: Geol. Soc. Am. Abstracts with Programs, v. 14, no. 1-2, pp. 88-89.

Taylor, L. A., 1978, A computer program for recalculating total FeO to obtain Fe^{2+} and Fe^{3+} as oxides: Unpublished manuscript, Univ. of Tennessee.

Thayer, P. A., 1967, Geology of the Dan River and Davie County Triassic basins, North Carolina: Unpublished Ph.D. dissertation, Univ. of North Carolina at Chapel Hill, 178 p.

Thayer, P. A., 1970, Geology of the Davie County Triassic basin, North Carolina: Southeastern Geol., v. 11, pp. 187-198.

United States Dept. of Agriculture, 1972, Soils in Davie County, North Carolina: U.S.D.A. Soil Conservation Serv. Pub. 4-R-26, 671-A.

Van der Plas, L., and Tobi, A. C., 1965, A chart for judging the reliability of point counting results: Am. Jour. of Science, v. 263, pp. 87-90.

Vejnar, A., 1975, Hornblende and problems of recrystallization of gabbroic rocks: Lithos, v. 8, pp. 59-68.

Wagener, H. D., 1974, The York-Chester gabbro-metagabbro-amphibolite complex: S. C. Div. of Geol. Geologic Notes, v. 18, pp. 1-3.

Waskom, J. D., and Bulter, J. R., 1971, Geology and gravity of the Lilesville granite batholith, North Carolina: Geol. Soc. Am. Bull., v. 82, pp. 2827-2844.

Wilson, F. A., and Daniels, D. L., 1980, Simple Bougner gravity map of the Charlotte 1° x 2° quadrangle, N. C. and S. C.: U.S.G.S. Miscellaneous Investigation Series, Map I-1251-A.

APPENDIX

Table A-1 Electron Microprobe Analyses (Averaged): Amphibole

	3-15-3/1*(7)**	3-15-3/2*(5)	3-15-3/3*(5)	3-15-3/4*(6)	5-10-6/5(7)	5-10-6/8(8)	5-10-6/9(7)	6-11-8/2(5)	6-11-8/7(6)	6-13-8/2(5)	6-13-8/3(6)	6-14-10/1(6)
SiO_2	41.4 (1.1)+	54.4 (1.3)	40.7 (0.7)	41.0 (1.0)	41.7 (0.4)	41.7 (0.6)	41.1 (1.3)	42.5 (1.0)	42.4 (0.2)	41.2 (0.4)	40.9 (0.6)	42.6 (0.4)
TiO_2	3.03(0.12)	0.06(0.02)	2.89(0.23)	3.76(0.21)	3.63(0.26)	4.26(0.13)	4.14(0.10)	0.88(0.36)	1.54(0.08)	3.75(0.12)	3.28(0.20)	2.34(0.25)
Al_2O_3	12.7 (0.3)	2.48(0.59)	12.3 (0.3)	12.7 (0.3)	13.0 (0.5)	12.7 (0.3)	12.8 (0.6)	12.7 (0.4)	13.3 (0.4)	13.3 (0.2)	13.7 (0.4)	14.3 (0.5)
FeO	5.43(0.14)x	0.20(1.06)	5.11(0.26)	5.70(0.43)	7.38(0.39)	8.36(0.41)	8.05(0.30)	0.00(1.11)	3.60(0.23)	5.09(0.39)	3.51(0.26)	3.59(0.36)
Fe_2O_3xx	5.82	8.79	5.58	5.56	2.82	2.77	3.23	10.8	8.92	3.90	7.06	6.72
MnO	0.14(0.03)	0.28(0.09)	0.14(0.03)	0.11(0.03)	0.14(0.06)	0.18(0.03)	0.15(0.04)	0.18(0.03)	0.19(0.03)	0.16(0.04)	0.18(0.01)	0.14(0.03)
MgO	14.1 (0.2)	19.3 (0.6)	14.2 (0.4)	13.9 (0.3)	13.9 (0.3)	13.7 (0.1)	13.5 (0.3)	17.3 (1.0)	15.2 (0.3)	14.8 (0.2)	15.6 (0.6)	15.0 (0.4)
CaO	11.5 (0.1)	11.2 (0.8)	11.4 (0.2)	11.2 (0.2)	11.2 (0.2)	11.4 (0.1)	11.3 (0.2)	12.2 (0.5)	12.0 (0.4)	11.7 (0.2)	12.0 (0.6)	11.4 (0.2)
Na_2O	2.13(0.16)	0.45(0.08)	2.14(0.23)	2.33(0.24)	2.67(0.14)	2.79(0.09)	2.53(0.22)	2.40(0.11)	2.43(0.08)	2.72(0.08)	2.61(0.18)	2.46(0.16)
K_2O	0.88(0.02)	N.D.θ	0.84(0.02)	0.79(0.11)	0.85(0.06)	0.82(0.04)	0.95(0.10)	0.91(0.06)	0.96(0.06)	0.82(0.05)	0.80(0.06)	1.02(0.16)
Total	97.13	97.16	95.30	97.05	97.29	98.68	97.76	99.87	100.54	98.24	99.72	99.57
Si	6.057	7.593	6.063	6.013	6.103	6.049	6.029	6.000	6.004	5.969	5.833	6.035
Ti	0.333	0.005	0.324	0.414	0.399	0.465	0.457	0.094	0.164	0.409	0.352	0.250
Al^{IV}	1.943	0.407	1.937	1.987	1.897	1.951	1.971	2.000	1.996	2.031	2.147	1.965
Al^{VI}	0.752	0.001	0.222	0.213	0.343	0.221	0.236	0.118	0.221	0.236	0.143	0.420
Fe^{2+}	0.664	0.023	0.636	0.698	0.903	1.015	0.987	0.000	0.427	0.714	0.419	0.426
Fe^{3+}	0.641	0.924	0.625	0.613	0.310	0.303	0.357	1.148	0.951	0.425	0.758	0.717
Mn	0.017	0.033	0.018	0.014	0.017	0.022	0.019	0.022	0.023	0.020	0.022	0.017
Mg	3.084	4.013	3.159	3.038	3.027	2.974	2.944	3.636	3.214	3.196	3.308	3.171
Ca	1.799	1.670	1.821	1.752	1.759	1.774	1.778	1.843	1.822	1.812	1.835	1.729
Na	0.604	0.122	0.615	0.662	0.757	0.786	0.720	0.658	0.668	0.764	0.722	0.676
K	0.164	0.000	0.160	0.148	0.159	0.152	0.178	0.164	0.174	0.152	0.160	0.185
Total	15.558	14.792	15.584	15.552	15.674	15.712	15.676	15.683	15.664	15.728	15.719	15.591

	6-14-10/5(5)	6-14-10/6(8)	6-15-4/2(7)	6-15-4/3(6)	6-15-5/5(5)	6-15-5/10(5)	8-4-58*/1(6)	8-4-58/2*(6)	9-60-5/1*(8)	9-60-5/2*(7)	9-60-5/3*(6)	9-60-5*/4(5)
SiO_2	42.1 (0.4)	41.6 (0.3)	40.6 (0.6)	40.8 (0.5)	41.6 (0.7)	42.1 (0.4)	41.0 (1.4)	41.5 (0.7)	45.0 (0.8)	51.4 (1.6)	45.6 (0.8)	52.9 (2.8)
TiO_2	2.45(0.12)	2.12(0.03)	3.68(0.08)	49(0.35)	3.77(0.31)	4.01(0.18)	1.77(0.31)	2.12(0.05)	2.35(0.64)	0.28(0.15)	1.88(0.31)	0.17(0.03)
Al_2O_3	13.5 (0.5)	13.1 (0.6)	12.4 (0.3)	13.9 (0.3)	14.1 (1.0)	12.5 (0.5)	13.0 (0.5)	13.4 (0.6)	10.8 (0.7)	6.23(1.15)	10.9 (0.6)	6.43(1.02)
FeO	5.75(0.88)	4.61(0.95)	8.08(0.19)	6.91(0.53)	6.23(0.49)	8.47(0.18)	1.05(0.30)	1.90(0.41)	6.84(0.50)	1.22(0.44)	5.66(0.32)	4.19(0.65)
Fe_2O_3xx	4.30	5.72	4.23	4.32	4.29	2.54	9.04	8.58	5.65	10.4	6.96	6.28
MnO	0.14(0.04)	0.14(0.03)	0.14(0.03)	0.17(0.03)	0.19(0.03)	0.14(0.04)	0.11(0.03)	0.17(0.03)	0.14(0.04)	0.29(0.05)	0.24(0.04)	0.32(0.03)
MgO	14.2 (0.5)	14.3 (0.5)	13.3 (0.2)	13.5 (0.4)	14.1 (0.4)	13.5 (0.2)	15.6 (0.4)	15.6 (0.5)	13.9 (0.5)	11.1 (0.8)	13.9 (0.6)	16.6 (0.5)
CaO	11.3 (0.3)	11.1 (0.3)	11.2 (0.2)	11.4 (0.2)	11.3 (0.2)	11.2 (0.3)	11.9 (0.4)	11.9 (0.2)	11.7 (0.1)	11.2 (0.3)	11.3 (0.3)	11.4 (0.3)
Na_2O	2.38(0.12)	2.28(0.14)	2.62(0.07)	2.26(0.12)	2.02(0.15)	2.70(0.07)	1.76(0.19)	2.09(0.15)	1.15(0.11)	0.68(0.15)	1.19(0.08)	0.79(0.08)
K_2O	1.13(0.11)	1.12(0.08)	1.05(0.11)	1.34(0.06)	0.80(0.07)	0.81(0.07)	0.60(0.07)	0.65(0.04)	0.86(0.19)	0.04(0.02)	0.70(0.18)	0.05(0.02)
Total	97.25	96.09	97.30	98.09	99.20	97.97	95.83	97.91	98.39	98.8	98.33	99.13
Atoms/23 (O, OH, F)												
Si	6.129	6.124	6.014	5.946	5.965	6.143	6.005	5.970	6.470	7.142	6.529	7.323
Ti	0.268	0.235	0.410	0.383	0.406	0.440	0.195	0.229	0.254	0.029	0.203	0.018
Al^{IV}	1.871	1.876	1.986	2.054	2.035	1.857	1.995	2.030	1.530	0.858	1.471	0.677
Al^{VI}	0.451	0.405	0.178	0.335	0.348	0.288	0.253	0.248	0.309	0.163	0.375	0.373
Fe^{2+}	0.700	0.568	1.000	0.843	0.747	1.033	0.129	0.229	0.823	0.142	0.678	0.485
Fe^{3+}	0.471	0.634	0.471	0.474	0.463	0.279	0.997	0.929	0.612	1.087	0.750	0.654
Mn	0.017	0.017	0.018	0.021	0.023	0.017	0.014	0.021	0.017	0.034	0.029	0.038
Mg	3.091	3.139	2.924	2.943	3.013	2.943	3.412	3.344	2.978	2.543	2.965	3.433
Ca	1.760	1.748	1.778	1.789	1.736	1.742	1.866	1.841	1.801	1.675	1.735	1.691
Na	0.672	0.652	0.752	0.639	0.784	0.763	0.500	0.583	0.321	0.183	0.331	0.212
K	0.210	0.211	0.198	0.249	0.146	0.151	0.112	0.119	0.158	0.007	0.128	0.009
Total	15.640	15.609	15.729	15.676	15.666	15.656	15.478	15.543	15.273	14.863	15.194	14.913

	9-60-5*/3(6)	9-60-5*/6(6)	9-60-7A*/1(6)	9-60-7A*/2(6)	9-60-7A*/3(5)	9-60-7C*/2(6)	9-60-7C*/3(8)
SiO_2	49.6 (1.6)	52.7 (3.8)	44.3 (0.7)	45.7 (1.0)	45.0 (0.9)	43.4 (1.1)	42.9 (0.6)
TiO_2	0.17(0.02)	0.23(0.17)	1.40(0.12)	1.34(0.03)	1.42(0.08)	2.48(0.08)	3.03(0.68)
Al_2O_3	8.44(2.14)	6.15(2.70)	8.86(0.55)	8.27(0.36)	8.32(0.25)	10.5 (0.3)	11.1 (0.4)
FeO	1.90(0.53)	2.32(1.14)	11.8 (0.8)	12.9 (0.8)	12.5 (0.4)	4.79(0.31)	6.18(0.27)
Fe_2O_3xx	9.89	8.91	4.66	3.79	3.43	5.59	5.49
MnO	0.23(0.05)	0.23(0.04)	0.61(0.04)	0.61(0.04)	0.64(0.05)	0.09(0.04)	0.11(0.03)
MgO	15.8 (1.7)	16.7 (1.9)	11.6 (0.3)	11.6 (0.5)	11.4 (0.4)	14.7 (0.3)	13.9 (0.2)
CaO	10.5 (0.8)	10.9 (0.4)	11.5 (0.2)	11.5 (0.1)	11.1 (0.3)	11.5 (0.1)	11.4 (0.2)
Na_2O	0.94(0.24)	0.68(0.27)	1.57(0.12)	1.55(0.05)	1.66(0.08)	1.14(0.07)	1.28(0.05)
K_2O	0.08(0.04)	0.06(0.07)	1.07(0.08)	1.04(0.08)	1.03(0.05)	0.93(0.05)	0.98(0.02)
Total	97.95	98.88	97.37	98.30	96.50	95.12	96.37
Atoms/23 (O, OH, F)							
Si	6.980	7.295	6.620	6.763	6.766	6.418	6.316
Ti	0.018	0.024	0.157	0.149	0.161	0.276	0.366
Al^{IV}	1.020	0.705	1.380	1.237	1.234	1.582	1.684
Al^{VI}	0.379	0.299	0.181	0.206	0.241	0.246	0.235
Fe^{2+}	0.223	0.268	1.477	1.591	1.576	0.666	0.761
Fe^{3+}	1.047	0.929	0.524	0.422	0.388	0.701	0.609
Mn	0.027	0.027	0.077	0.076	0.082	0.014	0.014
Mg	3.306	3.451	2.582	2.555	2.553	3.038	3.044
Ca	1.639	1.613	1.843	1.591	1.795	1.801	0.805
Na	0.256	0.183	0.455	0.455	0.484	0.365	0.366
K	0.014	0.011	0.204	0.196	0.198	0.184	0.184
Total	14.910	14.806	15.500	15.231	15.478	15.379	15.354

*Metagabbro samples. Analyses are for igneous amphiboles.

**Number in parentheses is the number of analyses averaged.

+Metagabbro samples. Analyses are for metamorphic amphiboles.

++Value in weight percent oxides with standard deviation from the mean in parentheses.

xStandard deviation is for total Fe as FeO.

xxFe_2O_3 calculated.

θNot detectable; less than 0.03%.

Table A-2. Electron Microprobe Analyses (Averaged): Biotite

	5-10-6(2)*	6-15-4(5)	9-6Q-7A**(5)
SiO_2	38.1 (0.7)+	37.0 (0.3)	36.5 (0.4)
TiO_2	3.83(0.10)	4.60(0.59)	2.90(0.23)
Al_2O_3	13.8 (0.1)	16.5 (0.3)	14.4 (0.1)
FeO++	12.1 (0.9)	9.59(0.48)	18.1 (0.2)
MnO	N.D.x	N.D.	0.36(0.06)
MgO	17.5 (0.7)	18.1 (0.9)	12.8 (0.3)
CaO	0.43(0.60)	N.D.	N.D.
Na_2O	0.10(0.07)	0.06(0.01)	0.12(0.04)
K_2O	9.10(0.71)	9.38(0.12)	9.21(0.28)
Total	94.96	95.23	94.39
		Atoms/22 (O, OH, F)	
Si	5.626	5.381	5.607
Ti	0.424	0.499	0.333
Al	2.399	2.825	2.601
Fe	1.492	1.165	2.326
Mn	0.000	0.000	0.045
Mg	3.855	3.930	2.920
Ca	0.069	0.000	0.000
Na	0.028	0.013	0.031
K	1.710	1.737	1.803
Total	15.603	15.550	15.666

*Sample number. Number in parenthesis is the number of analyses averaged.

**Metagabbro sample.

+Value in weight percent oxides with standard deviation from the mean.

++FeO = Total Fe.

xNot detectable; less than 0.03%.

Table A-3. Electron Microprobe Analyses (Averaged): Clinopyroxene

	3-15-3*(5)**	5-10-6(14)	6-11-8(5)	6-13-8(6)	6-14-10(7)	6-15-4(6)	6-15-5(5)	8-4-5*(6)	9-6Q-5A*(5)	9-6Q-7A*(6)	9-6Q-7C*(6)
SiO_2	50.5 (0.5)+	51.3 (0.7)	51.8 (1.3)	51.3 (2.5)	51.2 (0.8)	50.6 (0.3)	51.3 (0.4)	49.9 (0.3)	52.8 (0.6)	51.8 (0.9)	51.0 (0.3)
TiO_2	0.67(0.03)	0.87(0.07)	0.74(0.08)	0.90(0.08)	0.60(0.13)	0.70(0.07)	0.88(0.07)	0.50(0.03)	0.30(0.02)	0.34(0.26)	0.63(0.07)
Al_2O_3	4.04(0.11)	3.55(0.28)	3.71(0.19)	3.84(0.17)	4.26(0.28)	2.95(0.13)	3.37(0.13)	4.52(0.08)	2.00(0.09)	1.61(0.40)	3.16(0.21)
FeO^{++}	7.02(0.36)	7.28(0.53)	7.80(0.57)	7.57(0.66)	7.12(0.44)	8.45(0.21)	7.15(0.14)	7.78(0.39)	7.82(0.14)	9.23(0.58)	7.95(0.35)
MnO	0.24(0.04)	0.24(0.04)	0.22(0.05)	0.17(0.03)	0.22(0.03)	0.31(0.03)	0.27(0.05)	0.23(0.05)	0.17(0.03)	0.86(0.06)	0.11(0.05)
MgO	15.7 (0.5)	15.1 (0.4)	15.2 (0.2)	15.4 (0.6)	15.0 (0.3)	15.7 (0.5)	14.9 (0.2)	15.6 (0.2)	15.1 (0.1)	13.9 (0.4)	14.7 (0.2)
CaO	20.7 (0.8)	20.8 (0.9)	20.4 (0.6)	19.4 (1.0)	21.7 (0.8)	21.5 (0.5)	21.1 (0.8)	20.0 (0.2)	21.5 (0.3)	20.9 (1.0)	21.4 (0.7)
Na_2O	0.63(0.03)	0.57(0.08)	0.59(0.08)	0.62(0.07)	0.61(0.05)	0.59(0.01)	0.70(0.03)	0.47(0.05)	0.43(0.05)	0.75(0.05)	0.50(0.05)
Total	99.50	99.71	100.46	99.20	100.71	100.81	99.67	99.00	100.12	99.39	99.45
						Atoms/6 Oxygen					
Si	1.874	1.900	1.901	1.901	1.883	1.887	1.905	1.868	1.954	1.954	1.905
Ti	0.018	0.023	0.020	0.025	0.016	0.020	0.024	0.013	0.007	0.009	0.017
Al	0.176	0.154	0.160	0.167	0.184	0.128	0.147	0.198	0.086	0.071	0.138
Fe	0.216	0.225	0.239	0.233	0.218	0.261	0.221	0.242	0.241	0.290	0.248
Mn	0.006	0.006	0.006	0.004	0.006	0.010	0.007	0.006	0.004	0.026	0.003
Mg	0.866	0.833	0.834	0.849	0.818	0.865	0.821	0.869	0.831	0.779	0.816
Ca	0.821	0.826	0.800	0.769	0.855	0.852	0.839	0.799	0.849	0.844	0.857
Na	0.044	0.040	0.041	0.043	0.043	0.042	0.049	0.034	0.030	0.054	0.036
Total	4.021	4.007	4.001	3.991	4.023	4.055	4.013	4.029	4.002	4.027	4.020

*Metagabbro samples.

**Number in parentheses is the number of analyses averaged.

+Value in weight percent oxides with standard deviation from the mean value in parentheses.

++FeO = Total Fe.

xNot detectable; less than 0.03%.

Table A-4. Electron Microprobe Analyses (Averaged): Olivine

	5-10-6(5)*	6-11-8(6)	6-13-8(6)	6-14-10(6)	6-15-4(6)	6-15-5(9)	8-4-5**(6)
SiO_2	37.7 (0.6)+	38.3 (0.8)	37.4 (0.4)	38.3 (0.5)	36.5 (0.4)	38.2 (0.3)	38.2 (1.2)
FeO^{++}	24.0 (0.3)	17.0 (0.3)	20.3 (0.5)	21.8 (0.3)	26.7 (0.3)	23.7 (0.3)	17.5 (0.3)
MnO	0.48(0.06)	0.47(0.03)	0.35(0.05)	0.39(0.05)	0.43(0.03)	0.47(0.01)	0.41(0.04)
MgO	37.7 (0.2)	44.4 (0.3)	42.0 (0.4)	39.1 (0.2)	37.1 (0.3)	38.6 (0.3)	44.2 (0.5)
Total	99.88	100.07	100.05	99.59	100.73	100.97	100.31
				Atoms/4 Oxygen			
Si	0.995	0.973	0.967	0.996	0.967	0.991	0.973
Fe	0.528	0.361	0.438	0.474	0.591	0.514	0.372
Mn	0.010	0.007	0.007	0.008	0.009	0.010	0.008
Mg	1.469	1.682	1.618	1.522	1.464	1.494	1.674
Total	3.001	3.024	3.030	3.000	3.031	3.008	3.025

*Sample number. Number of analyses in parentheses.

**Metagabbro sample.

+Weight percent oxide. Number in parentheses is the standard deviation.

++FeO = Total Fe.

Table A-5. Electron Microprobe Analyses (Averaged): Orthopyroxene

	5-10-6(6)*	6-11-8(5)	6-13-8(6)	6-14-10(6)	6-15-4(5)	6-15-5(6)	8-4-5**	9-6Q-7C**
SiO_2	54.0 (0.8)+	54.1 (0.9)	54.6 (0.3)	54.6 (0.5)	54.0 (0.4)	55.0 (0.3)	53.9 (0.4)	53.3 (0.9)
TiO_2	0.24(0.07)	0.05(0.02)	0.17(0.03)	0.21(0.07)	0.29(0.03)	0.36(0.05)	0.17(0.03)	0.32(0.17)
Al_2O_3	2.00(0.13)	2.11(0.06)	2.50(0.17)	2.79(0.08)	2.02(0.08)	1.92(0.11)	2.91(0.08)	1.72(0.13)
FeO^{++}	15.3 (0.3)	14.1 (0.4)	14.0 (0.3)	14.0 (0.2)	17.4 (0.3)	15.1 (0.3)	14.1 (0.2)	19.2 (0.6)
MnO	0.48(0.08)	0.41(0.05)	0.38(0.04)	0.37(0.04)	0.44(0.03)	0.41(0.03)	0.33(0.05)	0.49(0.37)
MgO	27.6 (0.3)	29.3 (0.2)	28.1 (0.3)	28.8 (0.2)	26.6 (0.2)	28.3 (0.4)	28.4 (0.3)	24.7 (0.5)
CaO	1.02(0.60)	0.74(0.03)	0.88(0.14)	0.86(0.15)	1.05(0.13)	1.07(0.32)	1.09(0.17)	1.41(0.95)
Total	100.64	100.81	100.63	101.63	101.80	102.16	100.90	101.14
					Atoms/6 Oxygen			
Si	1.936	1.924	1.942	1.921	1.930	1.937	1.916	1.938
Ti	0.006	0.001	0.004	0.005	0.007	0.009	0.004	0.008
Al	0.084	0.087	0.104	0.114	0.084	0.080	0.122	0.073
Fe	0.458	0.417	0.417	0.411	0.521	0.444	0.418	0.583
Mn	0.014	0.011	0.010	0.010	0.012	0.011	0.009	0.015
Mg	1.472	1.556	1.489	1.513	1.417	1.483	1.501	1.338
Ca	0.039	0.027	0.033	0.032	0.040	0.040	0.041	0.054
Total	4.007	4.024	4.000	4.006	4.011	4.005	4.010	4.009

*Sample number with number of analyses in parentheses.

**Metagabbro samples.

+Values in weight percent oxides. The standard deviation from the mean value is in parentheses.

++FeO = Total Fe.

Table A-6. Electron Microprobe Analyses (Averaged): Plagioclase

	3-15-3*(6)**	5-10-6(6)	6-11-8(6)	6-13-8(6)	6-14-10(6)	6-15-4(6)	6-15-5(6)	8-4-5*(7)	9-6Q-5A*(6)	9-6Q-7A*(6)	9-6Q-7C*(5)
SiO_2	52.2 (0.5)+	54.5 (0.8)	52.2 (1.0)	52.2 (0.3)	52.6 (0.4)	54.8 (2.1)	53.3 (018)	46.6 (0.7)	53.8 (1.0)	62.3 (3.3)	51.7 (1.0)
Al_2O_3	29.9 (0.4)	28.3 (0.5)	30.1 (0.4)	29.9 (0.3)	29.4 (0.4)	29.1 (0.9)	29.5 (0.6)	33.8 (0.7)	28.9 (0.7)	23.9 (1.5)	30.3 (0.7)
CaO	12.6 (0.4)	11.0 (0.3)	12.0 (0.4)	11.9 (0.4)	11.8 (0.3)	11.3 (0.9)	11.6 (0.5)	16.7 (0.5)	11.2 (0.6)	5.54(1.72)	12.5 (0.7)
Na_2O	4.17(0.15)	4.86(0.12)	4.43(0.20)	4.29(0.15)	4.56(0.23)	4.84(0.63)	4.97(0.28)	1.71(0.31)	4.91(0.39)	8.06(1.02)	4.39(0.50)
K_2O	0.04(0.01)	0.18(0.04)	0.16(0.02)	0.16(0.02)	0.11(0.02)	0.21(0.05)	0.07(0.01)	N.D.x	0.04(0.01)	0.23(0.24)	0.18(0.05)
FeO++	0.26(0.05)	0.18(0.14)	0.21(0.04)	0.26(0.10)	0.14(0.08)	0.13(0.05)	0.18(0.05)	0.37(0.06)	0.11(0.10)	0.11(0.06)	0.23(0.05)
Total	99.17	99.02	99.10	98.71	98.61	100.38	99.62	99.18	98.96	100.14	99.30
						Atoms/8 Oxygens					
Si	2.386	2.478	2.385	2.392	2.410	2.459	2.419	2.156	2.448	2.754	2.364
Al	1.610	1.517	1.618	1.617	1.589	1.541	1.579	1.845	1.552	1.247	1.634
Ca	0.615	0.537	0.588	0.583	0.577	0.542	0.560	0.827	0.544	0.262	0.610
Na	0.369	0.429	0.391	0.380	0.405	0.420	0.437	0.152	0.433	0.690	0.389
K	0.001	0.009	0.008	0.008	0.005	0.012	0.004	0.000	0.001	0.011	0.009
Fe	0.009	0.006	0.008	0.009	0.005	0.004	0.006	0.013	0.004	0.003	0.008
Total	4.990	4.976	4.998	4.990	4.992	4.979	5.004	4.993	4.982	4.967	5.014

*Metagabbro samples.

**Number in parentheses is the number of analyses averaged.

+Value in weight percent oxides with standard deviation from the mean value in parentheses.

++FeO = Total Fe.

xNot detectable; less than 0.03%.

VITA

James Thomas Harden was born in Mobile, Alabama, on November 12, 1955. He graduated from Murphy Senior High School, Mobile, Alabama, in June 1974. He attended the University of South Alabama where he received a Bachelor of Science degree in Geology in June 1978. Having accepted a teaching assistantship, he entered the University of Tennessee, Knoxville, in September 1978. He received a Master of Science degree in Geology in December 1984.

The author is a member of the Geological Society of America, American Association of Petroleum Geologists, and Sigma Gamma Epsilon (a geology honorary society). Mr. Harden is presently working as a Petroleum Geologist for the Gulf Oil Corporation in Houston, Texas.

He is married to the former Marsha Ann Jemison of Mobile, Alabama.

GEOLOGIC MAP OF THE FARMINGTON GABBRO-METAGABBRO COMPLEX, NORTH CAROLINA

★ NORITE

☆ GABBRONORITE

✪ METAGABBRO PROTOLITH

* TYPE I METAGABBRO

● TYPE II METAGABBRO

x TYPE III METAGABBRO

CONTACTS, DASHED WERE INFERRED.

D/U FAULT, U-UPTHROWN D-DOWNTHROWN

GEOLOGY BY JAMES T. HARDEN

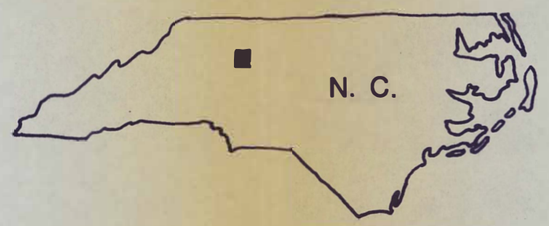

CONTOUR INTERVAL 10 FEET
DATUM IS MEAN SEA LEVEL